Journal of Contaminant Hydrology 276 (2026) 104779

Contents lists available at ScienceDirect

Journal of Contaminant Hydrology

journal homepage: www.elsevier.com/locate/jconhyd

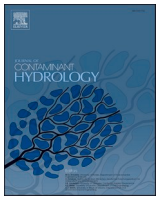

Modeling the fate of organic micropollutants in agricultural soils: Laboratory parameterization and field-scale implications

Mogens Thalmann [a,b,*], Sondra Klitzke [c], Andrea Lange [a,d], Aki Sebastian Ruhl [b,e], Andre Peters [a,f]

[a] Institute for Geoecology, Technische Universität Braunschweig, Langer Kamp 19c, 38106 Braunschweig, Germany
[b] German Environment Agency, Section II 3.3, Water Treatment, Schichauweg 58, 12307 Berlin, Germany
[c] German Environment Agency, Section II 3.1, Protection of Drinking Water Resources, Schichauweg 58, 12307 Berlin, Germany
[d] Thünen Institute of Rural Studies, Bundesallee 64, 38116 Braunschweig, Germany
[e] Technische Universität Berlin, Water Treatment, KF4, Str. des 17. Juni 135, 10623 Berlin, Germany
[f] Thünen Institute of Agricultural Technology, Bundesallee 50, 38116 Braunschweig, Germany

ARTICLE INFO

Keywords:
Organic micropollutants
Reclaimed water irrigation
Sorption kinetics
Microbial degradation
Inverse modeling
Field-scale transport
Hydrus-1D simulations

ABSTRACT

Organic micropollutants (OMP) increasingly enter agricultural soils through irrigation with reclaimed water, raising concerns about their mobility and persistence in soils and their potential to contaminate groundwater. This study investigates the fate of ten OMP in an arable loamy-sand topsoil using a combined experimental and modeling approach. Abiotic/biotic kinetic and isotherm batch experiments were performed to derive process-relevant parameters for sorption and biodegradation. An inverse modeling approach was employed to simultaneously fit the parameters for the different processes to all three data types (i.e., abiotic kinetic, biotic kinetic data, equilibrium data), allowing robust parameter estimation across varying levels of model complexity. The model incorporated equilibrium and kinetic sorption (linear and Freundlich isotherms; one- and two-site kinetic models), first-order biodegradation, and explicitly accounted for vaporization losses due to aerated vessels, extending traditional batch modeling frameworks.

Four OMP (adamantan-1-amine, carbamazepine, diclofenac, and sulfamethoxazole) exhibited biphasic sorption behavior, which was best described by a two-site kinetic model. Three OMP (acesulfame, saccharin, and valsartanate) showed negligible sorption but, following lag phases between 4 and 9 days, indicated microbial adaptation. After adaption, rapid biodegradation with half-lives of 0.4, 0.9, and 3.3 days, occurred. The remaining compounds (diatrizoate, trifluoromethanesulfonate, primidone) showed neither sorption nor degradation.

The necessity of applying the relatively complex modeling approaches — required to describe the lab experiments — to field conditions was investigated using Hydrus-1D simulations under realistic soil and climate scenarios. The simulations revealed that sorption kinetics and microbial adaptation phases had minimal impacts on OMP transport simulations at field-scale under matrix-dominated flow, despite their importance for laboratory-scale interpretation. The results suggest that simplified equilibrium and immediate-degradation assumptions may be sufficient for risk assessment regarding to OMP in homogeneous soils with predominantly uniform flow conditions.

Overall, this study presents a comprehensive framework for bridging laboratory observations with field-scale modeling, offering new insights into OMP fate and guiding efficient parameterization strategies for environmental risk assessment for the management of reclaimed water.

1. Introduction

The presence of organic micropollutants (OMP) in agricultural soils has become an increasing environmental concern, mainly due to irrigation with reclaimed water (RW) (Abdallat et al., 2022; Mora, and Torres-Martínez, J. A., Capparelli, M. V., Zabala, A., and Mahlknecht, J,

* Corresponding author at: Institute for Geoecology, Technische Universität Braunschweig, Langer Kamp 19c, 38106 Braunschweig, Germany.
E-mail address: m.thalmann@tu-braunschweig.de (M. Thalmann).

https://doi.org/10.1016/j.jconhyd.2025.104779
Received 13 June 2025; Received in revised form 19 September 2025; Accepted 16 November 2025
Available online 18 November 2025
0169-7722/© 2025 The Authors. Published by Elsevier B.V. This is an open access article under the CC BY license (http://creativecommons.org/licenses/by/4.0/).

2022). OMP, which include pharmaceuticals, personal care products, industrial chemicals, and pesticides might persist in RW because conventional wastewater treatment plants are not designed to effectively remove these contaminants (Luo et al., 2014; Belete et al., 2023). As a result, OMP continuously enter aquatic environments and agricultural soils through discharge of treated wastewater and RW crop irrigation (Margot et al., 2015; Bijlsma et al., 2021), respectively. Concerns regarding their environmental impact in agricultural soils include potential contamination of groundwater through leaching (Helmecke et al., 2020; Partyka and Bond, 2022), shifting soil physico-chemical properties as a result of long-term RW irrigation (Hashem and Qi, 2021; Ofori et al., 2024), and bioaccumulation in edible crops (Nguyen et al., 2023; Seelig et al., 2025).

Once introduced into soil, OMP undergo various physico-chemical and biological processes that determine their mobility, persistence, and ultimate fate (Nguyen et al., 2023; Pérez-Lucas and Navarro, 2024). Among these, sorption and microbial degradation are the dominant controls on OMP mobility and persistence under different water flow regimes (Qin et al., 2014; Ren et al., 2018; Gworek et al., 2021; Zhang et al., 2021).

Sorption involves the interaction between OMP and soil surfaces and can be described by both kinetic and equilibrium models (Chorover and Brusseau, 2008; Alhalabi et al., 2024). Equilibrium sorption models, such as linear or non-linear sorption isotherms, usually account for concentration-dependent sorption, while kinetic models describe time-dependent interactions. Sorption is affected by physico-chemical properties of OMP, soil characteristics, and solution matrix properties including pH, ionic strength, and dissolved organic carbon content (Xu et al., 2021; Alhalabi et al., 2024). Typically, sorption kinetics follow a biphasic pattern, with an initial rapid phase followed by a slower approach to equilibrium (Site, 2001; Alhalabi et al., 2024).

Microbial degradation plays a key role in the natural attenuation of many OMP, transforming or mineralizing them (Avisar et al., 2009; Gibson et al., 2010; Qin et al., 2014). The efficiency of biodegradation is enhanced by microbial adaptation to the specific OMP (Spain and Van Veld, 1983; Sandrin et al., 2001), favorable environmental conditions such as temperature, soil moisture, and redox status (Lin and Gan, 2011; Greskowiak et al., 2017; de Wilt et al., 2018), and active and diverse microbial communities often stimulated by organic matter inputs (Barra Caracciolo et al., 2015; Menacherry et al., 2023; Rietra et al., 2024). Conversely, unfavorable conditions such as anoxic milieu, low microbial abundance, or recalcitrant OMP structures can markedly reduce biodegradation efficiency. For instance, carbamazepine is well known for its persistence in soils due to its stable aromatic ring structure, limited functional groups for microbial attack, and resistance to enzymatic degradation (Grossberger et al., 2014). After the initial exposure of OMP to soil, the soil microbial communities may require time to express relevant degradative enzymes (Sandrin et al., 2001). The microbial adaption and corresponding lag phases reflected as delayed onset of OMP degradation are a common phenomenon in soils, and may substantially affect the fate of OMP in soils (Sandrin et al., 2001; Branco et al., 2023).

Traditional laboratory experiments under controlled conditions, such as batch and column studies, are essential for parameterizing sorption and biodegradation models (Banzhaf and Hebig, 2016). Accurately distinguishing between sorption and biodegradation requires a comparison of sterilized (abiotic) and unsterilized (biotic) systems (Hurtado et al., 2017; Lees et al., 2018; Schübl et al., 2021). Accurate estimation of biodegradation rates from batch experiments requires either comprehensive mass balance analyses via extraction and quantification of OMP from both solid and liquid phases, or explicitly accounting for sorption processes in the data modeling approach when only aqueous concentrations are measured.

Several well-established modeling approaches of different complexities enable accurate parameter estimation for both static (batch) and dynamic (flow-through columns) soil-water systems (van Genuchten and Wagenet, 1989; Streck et al., 1995). Heistermann et al. (2003) demonstrated the importance of sorption kinetics by integrating batch and column data to model the fate of the herbicide metsulfuron-methyl in loamy silt soil. Other studies investigating sorption and biodegradation of OMP in soil have similarly emphasized the relevance of sorption kinetics for correct evaluation of lab-scale data (e.g., Lee et al., 2014; Mutavdžić Pavlović et al., 2017; Luo et al., 2024).

While sorption kinetics play a crucial role in accurately interpreting laboratory data, their importance for field-scale transport under natural conditions is unclear. Given that most OMP exhibit relatively rapid sorption (Site, 2001; Alhalabi et al., 2024), kinetic limitations may be negligible at field-scale. Similarly, microbial adaptation, which potentially delay the onset of biodegradation, may have little effect on OMP transport at larger spatial and temporal scales. Accordingly, it remains unclear whether kinetic limitations and microbial adaptation, which strongly influence lab-scale interpretation, are equally relevant at the field scale or whether they average out under natural conditions. Addressing this knowledge gap is essential to improve the reliability of model-based risk assessments for OMP transport in agriculture, especially under irrigation with RW. We hypothesize that although kinetic limitations and microbial lag phases are essential for robust parameter estimation in batch experiments, their effect on OMP transport under field conditions may be negligible if they occur within typical environmental ranges.

To address these uncertainties, research is needed to bridge laboratory findings with field-scale processes by integrating experimentally derived parameters into OMP field-scale simulations. The aim of this study was to (i) investigate the fate of ten selected OMP (namely acesulfame, adamantan-1-amine, carbamazepine, diatrizoate, diclofenac, primidone, saccharin, sulfamethoxazole, trifluoromethanesulfonate, valsartanate) in an agricultural topsoil in context of irrigation with RW using an advanced measurement and modeling approach that accounts for sorption kinetics, non-linear sorption isotherms, and microbial degradation, including potential microbial adaptation phases, and (ii) assess the relevance of sorption kinetics and microbial adaptation phases for field-scale OMP transport modeling under realistic agricultural soil conditions, including contrasting climate and groundwater proximity scenarios. By explicitly combining inverse modeling of batch data with process-based simulations, this study provides a unique test of whether simplified model assumptions (instantaneous sorption, immediate biodegradation) remain reliable under simulated field conditions.

2. Material & methods

2.1. Geolocation and soil characteristics

Soil samples were collected in 10–20 cm depth of the topsoil horizon (0–30 cm) of a Stagnic Cambisol in an arable field located in Brandenburg, southwest of Berlin (northeast Germany, 52°16′34.3"N 13°04′39.7″E). The field undergoes periodic plowing, which influences soil structure and composition. The geological setting consists of a terminal moraine from the Weichselian glaciation, covered by bedload sand.

The freshly sampled soil material was stored at 8 °C covered with perforated cling film until use in batch experiments to maintain field moisture and preserve microbial community integrity as much as possible (Lees et al., 2018). Before the experiments, the soil was homogenized and sieved to grain sizes below 2 mm. Physico-chemical soil properties measured using standardized methodologies are presented in Table 1. Given the slightly acidic soil conditions, the calcium carbonate content is expected to be negligible.

2.2. Characteristics of examined organic micropollutants

A stock solution with nine of the ten examined OMP was prepared by dissolving 10 mg of each substance (all analytical grade) in 1 L of

Table 1
Physico-chemical properties of soil samples. C_{ORG} is the organic carbon content, EC the electrical conductivity, and CEC the cation exchange capacity representing the sum of exchangeable cations on the soil surfaces.

Textural fractions[1] (mass-%)			Texture class[2]	C_{ORG}[3]	pH[4]	EC[5]	CEC[6]
Sand	Silt	Clay		mass-%		µS cm^{-1}	mmol kg^{-1}
84.9	6.2	8.5	Loamy sand	1.47	5.2	62.9	25.4

[1] analyzed by the PARIO method (Durner and Iden, 2021)
[2] classification according to the USDA system (USDA, 2017)
[3] determined by combustion at 1350 °C with O_2 supply and subsequent absorption in a barium perchlorate solution and measured through titration of Ba$(OH)_2$ to the initial pH
[4] measured in 0.01 mol L^{-1} $CaCl_2$ solution with a soil solution ratio of 1:2.5
[5] measured in H_2O with a soil-to-water ratio of 1:10
[6] value adopted from analyzes of a topsoil sample of the same field (Thalmann et al., 2025a, 2025b)

ultrapure water (Milli-Q ® IQ 7000). The stock solution was stored at 8 °C until usage. TFMSA, which was not added to the stock solution was considered by its original concentration in the RW. Abbreviations, suppliers, and physico-chemical properties of all examined OPM are summarized in Table 2. OMP concentrations in aqueous samples collected in the experiments were analyzed using high-performance liquid chromatography (HPLC) coupled to a triple-quadrupole mass spectrometer (MS/MS), as described in detail by Zeeshan et al. (2023).

2.3. Water used in experiments

RW was used as the aqueous phase in both the kinetic and isotherm batch experiments (see below). The RW was collected from a large conventional wastewater treatment plant located in Berlin, which employs tertiary treatment and seasonal UV disinfection (May 1st to September 30th). Due to a four-month gap between the isotherm and kinetic batch experiments, two distinct RW batches were used for the respective experiments. Their characteristics are summarized in Table 3.

For the kinetic experiments, RW was collected outside the regular UV disinfection period and was therefore independently disinfected in the laboratory. This was achieved using a 254 nm UV lamp (UV-EL, Germany) placed in a stainless-steel reactor, as described in detail by Thor et al. (2025). While this procedure likely inactivated microorganisms, it also led to partial degradation of certain OMP due to the high applied UV dose, as confirmed by Thor et al. (2025). Consequently, concentrations of several OMP in the UV-treated RW used in the kinetic experiments were notably lower than in the RW used in the isotherm experiments (Table 3).

2.4. Experiments

2.4.1. Sorption isotherm experiments

The isotherm batch experiments were conducted following OECD (Organisation for Economic Co-operation and Development) 106 guidelines for sorption testing in batch systems (OECD, 2000). A soil-to-solution ratio of 1:2 was selected, consistent with previous batch sorption experiments using soil from the same location and a similar set of OMP (Thalmann et al., 2025a, 2025b). Before the experiment, the soil was air-dried. Considering its residual water content (1.8 mass-%), 7.13 g of soil and 13.87 mL of reclaimed water (RW) were added to 50 mL glass centrifuge tubes. Seven working solutions with different OMP concentration levels (around 0.5, 1.5, 5, 15, 50, 100, and 200 µg L^{-1}) were prepared by diluting a 10 mg L^{-1} stock solution in RW, with the spiked OMP adding to the original concentrations already present in RW. All soil-containing samples were prepared in triplicates. In addition, control samples without soil (containing 30 mL solution) were prepared in duplicate for each concentration level to assess OMP stability and potential adsorption to the vessel walls. To account for potential background contamination of the soil, blank samples (soil in 0.01 mol L^{-1} $CaCl_2$ without OMP) were run as triplicate. To inhibit microbial activity and prevent OMP biodegradation, 0.2 g L^{-1} sodium azide (NaN_3) was added to each sample, which is a common sterilization procedure (Lees et al., 2018). All tubes were shaken for 48 h on a horizontal shaker (IKA HS 501) at 230 rpm in the dark. A 48 h contact time was selected in line with recent sorption studies on similar soils and OMP (Thalmann et al., 2025a, 2025b; Chefetz et al., 2008; Rodríguez-López, and Santás-Miguel, V., Cela-Dablanca, R., Núñez-Delgado, A., Álvarez-Rodríguez, E., Pérez-Rodríguez, P., and Arias-Estévez, M, 2022; Rodríguez-López et al., 2024; Storck et al., 2016; Wu et al., 2020). Sorption kinetics of OMP in soils are typically much faster and generally approach equilibrium within a few hours, so that 48 h is expected to be sufficient to reach apparent equilibrium. At the same time, equilibration was not extended beyond 48 h because the effectiveness of NaN_3 to suppress microbial activity may decline over longer periods, potentially allowing biodegradation to resume. Subsequently, samples were immediately centrifuged at 2300 rpm for 30 min (Thermo Scientific Sorvall LYNX 6000). A 10 mL aliquot of the aqueous supernatant was then filtered through a 0.45 µm syringe filter (regenerated cellulose, Macherey-Nagel GmbH), discarding the first few milliliters and subsequently analyzed for OMP concentrations.

2.4.2. Kinetic experiments

The kinetic batch experiments were conducted following the approach of Martinez-Hernández et al. (2016). A total of 504.1 g of field-moist soil (10.7 mass-% water contentTable 1) was weighed into two-liter glass bottles and mixed with 1293.2 mL of RW (batch KIN in Table 2), resulting in a final soil-to-solution ratio of 1:3 (i.e., 450 g solid soil and 1350 mL solution). To differentiate between sorption and microbial degradation, three abiotic batches containing 0.2 g L^{-1} NaN_3 to inhibit microbial activity and three biotic vessels without NaN_3 were prepared. In the abiotic vessels, only sorption was expected to occur, while the biotic vessels allowed to observe coupled sorption and biodegradation. Additionally, blank samples (1293.2 mL of 0.01 mol L^{-1} $CaCl_2$ with 504.1 g soil) and control samples (300 mL spiked RW without soil in 500 mL glass vessels) were included in both abiotic and biotic variants.

To allow pre-equilibration between soil and solution, all soil-containing vessels were shaken for 17 h before spiking the 10 mg L^{-1} OMP stock solution, which added 20 µg L^{-1} to the original OMP concentrations in the RW (Table 2). However, during this pre-equilibration phase, original OMP were subject to sorption and/or biodegradation, which had to be accounted for in the modeling approach. All vessels were continuously shaken in the dark at 25 ± 1 °C on a horizontal shaker (circular motion; IKA KS 501) at 140 rpm. To maintain aerobic conditions, bottles remained uncapped throughout the experiment, leading to vaporization and a gradual decrease of solution volume and hence a change in soil-to-solution ratio during the experiment. Vaporization losses were monitored by regularly weighing the vessels (3 times during first spike experiment), which was considered in subsequent data modeling.

Aliquots of 3.5 mL were sampled at 12 times (0.5, 1.25, 2.5, 4, 6, 8, 11, 24, 48, 72, 144, 240, and 312 h), removing a total of 4.2 % of the initial volume by the end of the experiment. Following the final sampling of the first OMP spike, all biotic vessels were refilled to the initial volume with RW (batch KIN in Table 3) to compensate for losses due to evaporation and sampling, while blanks were refilled again with 0.01 $CaCl_2$ solution. In accordance with Martinez-Hernández et al. (2016), a second OMP spike was added subsequently to this final sampling, and serial sampling was repeated at similar times (0.5, 1.25, 2.5, 4, 6, 8, 11, 24, 48, 72, 144, 216, and 336 h). This extended sampling period for the biotic vessels was included to investigate potential lag phases associated with microbial adaptation. Again, all samples were analyzed for OMP concentrations using the prior described HPLC-MS/MS method.

Table 2
Physico-chemical properties of examined OMP, including abbreviations, suppliers (SP), usage, molecular weight, octanol-water distribution coefficient (logD at pH 7.5). The last column shows the molecular structures with pKa values for corresponding functional groups. More detailed information on OMP is given by Zeeshan et al., 2023.

OMP	Abbreviation	SP	Usage	Molecular weight (g mol^{-1})	Charge at pH 7.5	logD[a] at pH 7.5	Structure with pK_a values at corresponding functional groups
Acesulfame	ACE	S	Artificial sweetener[b]	201.24	negative	−3.06	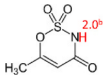
Adamantan-1-amine	ATA	F	Influenza A virus medication, anti-Parkinson agent[c]	151.25	positive	−1.35	
Carbamazepine	CBZ	S	Antiepileptic[e]	236.27	neutral	2.95	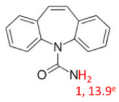
Diatrizoate	DZA	S	X-ray contrast compound[f]	613.93	negative	−0.63	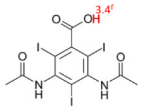
Diclofenac	DCF	S	Analgesic[g]	296.15	negative	1.05	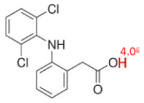
Primidone	PRI	S	Anticonvulsant[h]	218.25	neutral	1.12	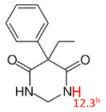
Saccharin	SAC	S	Artificial sweetener[i]	183.18	negative	−0.49	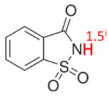
Sulfamethoxazole	SMX	S	Antibiotic[j]	253.28	negative	−0.08	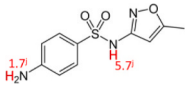
Trifluoromethanesulfonate	TFMSA	–	Short chained PFAS with diverse usage[k]	150.08	negative	−1.23	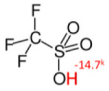
Valsartanate	VSA	B	Main metabolite of the antihypertensive drug valsartan[l]	266.25	2× negative	−1.35	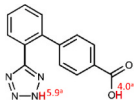

Suppliers: S Sigma-Aldrich, F Fluorochem, B Biozol
[a](Chemaxon, 2025), [b](Belton et al., 2020), [c](Ghosh et al., 2010), [e](Schmidtová et al., 2020), [f](Lerner, 1975), [g](Lara-Pérez et al., 2020), [h](Schaffer et al., 2012), [i](Buerge et al., 2010), [j](Xu et al., 2018), [k](Ali et al., 2022), [l](Huntscha et al., 2012)

Table 3
Concomitant chemical parameters and OMP concentrations in RW batches used in either batch experiments. ISO is the RW batch used in the isotherm experiments, and KIN the UV-treated RW batch used in the kinetic experiments. "<LQ" refers to values below the analytical limit of quantification and "n.a." indicates "not analyzed". OMP concentrations are given as original concentrations before spiking.

Batch	Concomitant parameters			Organic Micropollutants (µg L^{-1})									
	pH	EC (µS cm^{-1})	DOC (mg L^{-1})	ACE	ATA	CBZ	DCF	DZA	PRI	SAC	SMX	TFMSA	VSA
ISO	7.3	951	n.a.	0.70	0.19	1.05	4.64	2.68	0.43	0.09	0.23	0.01	1.34
KIN	7.1	1216	13.5	0.01	0.15	0.86	<LQ	<LQ	0.37	0.14	0.07	0.07	3.19

2.5. Concomitant parameters

Electrical conductivity (EC), pH, and dissolved organic carbon (DOC) were monitored during kinetic batch experiments and pH and EC at the end of the isotherm experiments to assess matrix conditions and potential side effects, as displayed in Fig. S1 provided in the supplementary information (SI). In the biotic samples, pH slightly decreased, while abiotic soil samples showed a slight increase, likely due to NaN_3

addition, which is known to elevate pH in soil suspensions (Lees et al., 2018; Süßmuth et al., 2024). A gradual EC increase in all vessels, due to evaporative ion up-concentration was observed. DOC concentrations in biotic soil samples remained stable (ca. 20 mg L^{-1}), suggesting limited microbial turnover. In contrast, DOC increased strongly in abiotic samples, reaching up to 65 mg L^{-1}, indicating enhanced leaching of organic matter caused by NaN_3.

3. Inverse modeling and field simulations

3.1. Conceptual model approach

We used the conceptual two-side sorption model described by van Genuchten and Wagenet (1989) combined with a first order degradation model (Fig. 1A with its compartments). In this model, the soil has two types of sorption sites: (i) a fraction of sites where sorption is instantaneous (equilibrium sites, often denoted s_1), and (ii) the remaining sites where sorption is kinetically limited (non-equilibrium sites, s_2).

Microbial degradation is assumed to occur only in the aqueous phase (solution), which includes biofilms. Negligible degradation in the sorbed phase is a legit simplification according to van Genuchten and Wagenet (1989) and to a review by Katayama et al. (2009). Because our kinetic batch experiments were conducted in open, continuously shaken vessels, we extended the model to account for water loss (vaporization) over time. Water losses are also highly relevant for irrigation. Fig. 1B schematically depicts this extension, where a volume loss from the solution compartment leads to a gradually increasing soil–solution ratio. This vaporization process is represented as a constant (zero-order) rate process, as detailed below. Vaporization rate constants γ [Lh^{-1}] were estimated based on three weight measurements of all vessels along the first spike experiment (Fig. S1).

3.2. Model components

We combined four basic process descriptions to build a coupled equation system combining all relevant processes. The model equations for each process are formulated and explained in detail in Table 4. Sorption equilibrium was described using either a linear Henry or a non-linear Freundlich isotherm. Sorption kinetics were incorporated in two alternative ways: a one-site kinetic model (all sorption is time-dependent with a single first-order rate; $s_1 = 0$ in Fig. 1A) and a two-site kinetic model (full model in Fig. 1A).

3.3. Governing coupled equation system

The coupled system of equations was derived by combining the above-described components as summarized and explained in Table 4 (a full derivation is provided in Appendix A1). Below we present the governing equations for the most complex case combining a non-linear Freundlich isotherm with two-site sorption kinetics, noting that the simpler models are special cases:

$$\frac{dV}{dt} = -\gamma \tag{1}$$

$$s_{eq}(c) = k_f c^n \tag{2}$$

$$\frac{dc}{dt} = -\frac{(kV-\gamma)\,c + m\alpha\left[(1-f)\,s_{eq}(c) - s_2\right]}{V + mfs_{eq}(c)'} \tag{3}$$

$$\frac{ds_2}{dt} = \alpha\left[(1-f)\,s_{eq}(c) - s_2\right] \tag{4}$$

Eq. (1) governs the solution volume decline due to vaporization. Eq. (2) represents the Freundlich sorption isotherm relating the instantaneous sorbed concentration and/or the equilibrium sorbed concentration to the current aqueous concentration. In case $n = 1.00$, it simplifies to a linear Henry isotherm. Eqs. (3) and (4) describe the OMP concentration change in the aqueous phase and the kinetic sorption dynamics on the kinetically limited sorption sites (s_2-sites), respectively. The term $s_{eq}(c)'$ in Eq. (3) represents the first derivative of Eq. (2). The coupled equation system reduces to a one-site kinetic sorption model (Table 4) if $f = 0$ (all sorption is kinetic), or to an instantaneous equilibrium model if $f = 1$. In case of no degradation, the term kV in Eq. (3) diminishes.

The coupled system of differential equations (Eqs. (1) to (4)) was numerically solved using MATLAB's built-in ordinary differential equation solvers (version R2023b; MathWorks, 2023).

3.4. Optimization procedure and objective function

We simultaneously fitted the coupled models summarized in Eqs. (1) to (4) to the three experimental data sets: 1) the sorption equilibrium isotherm data (only Eq. (2)), 2) the abiotic kinetic batch data (the term kV in Eq. (3) is zero), and iii) the biotic kinetic batch data (data of first OMP spike). The objective function was defined as the sum of weighted squared residuals between measured and modeled values for all data points across the three experiments:

$$\Phi(\theta) = w_{Iso}\sum_{i=1}^{n_{Iso}}\left[s_{eq,i}^{obs} - s_{eq,i}^{mod}(\theta)\right]^2 + w_{Kin}\sum_{i=1}^{n_{Kin}}\left[c_j^{obs} - c_j^{mod}(t_j,\theta)\right]^2 + w_{Deg}\sum_{i=1}^{n_{Deg}}\left[c_k^{obs} - c_k^{mod}(t_k,\theta)\right]^2 \tag{5}$$

where θ denotes the parameter vector specific to each model configuration (see below; Table 5). $s_{eq,i}^{obs}$ and $s_{eq,i}^{mod}$ refer to the observed and modeled sorbed concentration from the isotherm experiment. c_j^{obs} and c_j^{mod} are observed and modeled concentrations in abiotic batches (sorption kinetics) at time t_j, and c_k^{obs} and c_k^{mod} are observed and modeled concentrations for the biotic batches (coupled sorption and biodegradation kinetics) at time t_k. n_{Iso}, n_{Kin}, and n_{Deg} are the respective numbers

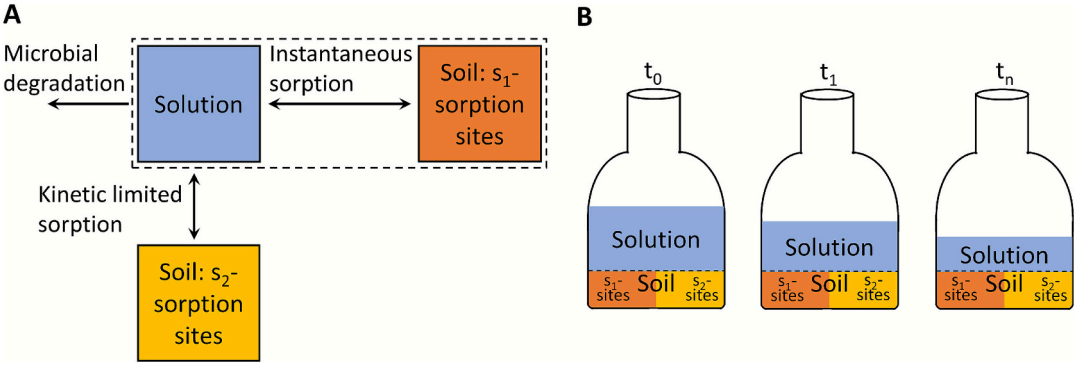

Fig. 1. Conceptual compartment model for batch experiments (A), and concept of changing soil-solution-ratio due to vaporization of kinetic batch experiment (B).

Table 4
Governing equations for the relevant processes of OMP in the soil batch experiments.

Process	Model	Governing equation	Explanation
Vaporization	zero-order	$\frac{dV}{dt} = -\gamma$	$V(t)$ [L] is the time-dependent liquid volume; t [h] is the time; γ [L h^{-1}] is the vaporization rate constant
Microbial degradation	first-order	$\frac{dc}{dt} = -k\,c$	$c(t)$ [µg L^{-1}] is the concentration in solution at time t; k [h^{-1}] is the first-order degradation rate constant
Sorption equilibrium	Henry (linear)	$s_{eq}(c) = k_d\,c$	$s_{eq}(c)$ [µg kg^{-1}] is the sorbed concentration in equilibrium state at concentration c; k_d[L kg^{-1}] is the linear distribution coefficient;
	Freundlich (non-linear)	$s_{eq}(c) = k_f c^n$	k_f[µg^{1-n} L^n kg^{-1}] is the Freundlich distribution coefficient; n [−] is the Freundlich exponent (restrained to values <1, as higher values lead to isotherms which are mechanistically not plausible)
Sorption kinetics	One-site sorption[1]	$\frac{ds}{dt} = \alpha\,(s_{eq}(c) - s)$	s [µg kg^{-1}] is the time-dependent kinetically limited sorbed concentration (similar to s_2-sites in Fig. 1A); α [h^{-1}] is the first-order kinetic rate constant
	Two-Site sorption[1]	$\frac{ds_1}{dt} = f s_{eq}' \frac{dc}{dt}$; $\frac{ds_2}{dt} = \alpha\left[(1-f)\,s_{eq}(c) - s_2\right]$	s_1 [µg kg^{-1}] is the sorbed concentration at s_1-sites (instantaneous); s_{eq}' [µg kg^{-1} h^{-1}]: first derivative of sorption isotherm with respect to c; f [−] is the fraction of s_1-sites; s_2 [µg kg^{-1}] is the time-dependent sorbed concentration at s_2-sites (kinetically limited)

[1] based on van Genuchten and Wagenet (1989)

Table 5
Four tested models as combinations of two isotherm (Henry and Freundlich) and two kinetic models (one-site and two-site). For parameters explanation see Table 4.

Model ID	Isotherm model	Kinetic model	Parameter set θ
OS-H	Henry	One-site	k_d, α, k
TS-H	Henry	Two-site	k_d, α, f, k
OS-F	Freundlich	One-site	k_f, n, α, k
TS-F	Freundlich	Two-site	k_f, n, α, f, k

of data points, given as means of triplicate measurements. w_{Iso}, w_{Kin}, w_{Deg} are weights used to balance the contributions of the individual data sets within the objective function. Specifically, the isotherm component w_{Iso} was heuristically assigned a weight of 0.1 accounting for the roughly one order of magnitude higher values of that data range. The resulting weighted objective function (Eq. (5(5)) was minimized using the trust-region-reflective algorithm, provided by the MATLAB Optimization Toolbox. To avoid misinterpretation of a local minimum, the optimization was repeated from multiple initial parameter sets, ensuring more robust identification of the global minimum.

For abiotic kinetic batches, only data in the first 48 h was used to be consistent with the equilibrium time applied in isotherm experiments. Moreover, NaN_3 may not inhibit biodegradation throughout the experiment, as also discussed in the study limitations (Section 4.4). By fitting all data at once, we obtain one set of parameters that optimally represents both equilibrium and time-dependent behavior, avoiding contradictions that might arise from separate fits.

3.5. Model selection

To avoid over-parameterization, we compared four model configurations of increasing complexity, combining either Henry or Freundlich isotherms with one-site or two-site kinetics (**Error! Reference source not found.**). We selected the most appropriate model system based on the lowest corrected Akaike Information Criterion (AIC_C) for small sample sizes (Hurvich and Tsai, 1989). In addition, the root mean square error (RMSE) between observed and simulated values was used as a supplementary measure of goodness-of-fit. This multi-dataset fitting procedure ensured that the selected model and parameter set could simultaneously reproduce the equilibrium isotherm, the sorption kinetics, and the biotic degradation kinetics. As a result, we obtain robust parameter estimates that are consistent across all observations. This approach aligns with a previous study that integrated batch and column data to comprehensively model sorption and degradation processes (Heistermann et al., 2003). The final calibrated models served as input for subsequent predictive field-scale simulations.

3.6. Field simulations

To evaluate the relative importance of sorption kinetics, and microbial adaption periods derived from laboratory experiments for simulated OMP transport at field-scale, process-based simulations were conducted using the Hydrus-1D (H1D) software package, version 4.17.0140 (Šimůnek et al., 2013). H1D numerically solves the Richards equation for variably saturated flow and the advection-dispersion equation for coupled solute transport in porous media as one-dimensional processes (Šimůnek and van Genuchten, 2008). The implemented chemical non-equilibrium models in H1D include both one-site and two-site kinetic formulations, as outlined in Section 3.2.

The general simulation setup in H1D, including the soil domain, boundary conditions, and climate scenarios, follows the modeling framework described by Thalmann et al. (2025a). The simulations represent a realistic agricultural cropping system irrigated with RW under site-specific conditions corresponding to the soil sampling site, characterized by a sandy loam texture, humid climate, demand-based irrigation, and a crop rotation system with winter wheat and phacelia (adopted from Feifel et al., 2024). The PDI model system (Peters et al., 2024) was used to describe the soil hydraulic properties of the specific site. Uptake by plants was not considered.

To test whether the effects of sorption kinetics and microbial lag phases depend on hydrologic setting, we used four combinations: (i) humid vs. semi-arid climate and (ii) a free-drainage lower boundary (deep groundwater) vs. a constant pressure head h = 0 cm at the lower boundary (shallow groundwater, i.e., a water table at 2 m below surface). All other inputs and parameters matched the base case (domain, soil hydraulic functions, transport and reaction parameters, management, and simulation periods). A full description of the simulation configurations is provided in the SI (Section S2.1).

To assess the relevance of sorption kinetics for field simulations, OMP exhibiting sorption were simulated using the most suitable kinetic model (i.e., one-site or two-site sorption), as determined by the lowest AIC_C value, and compared against a simple model assuming instantaneous equilibrium sorption.

To evaluate the effect of lag phases on field-scale transport simulations, we assumed that biodegradation is delayed for the individual observed OMP lag phases at the onset of the first RW irrigation event (first OMP input). This was achieved by splitting the simulation into two sequential runs: The initial run covered the “warm-up” phase until the first RW irrigation event plus the observed adaption period. Then the

final conditions of moisture and solute concentration distribution in the soil domain were taken as starting conditions for the second run, in which microbial degradation was activated according to the observed first-order biodegradation rates. These simulations were compared against the simple case in which degradation starts without lag-phase.

Microbial degradation is strongly affected by environmental factors, such as temperature, soil moisture, and soil depth among others (FOCUS, 2021; Naylor et al., 2022; Campan et al., 2023). A detailed

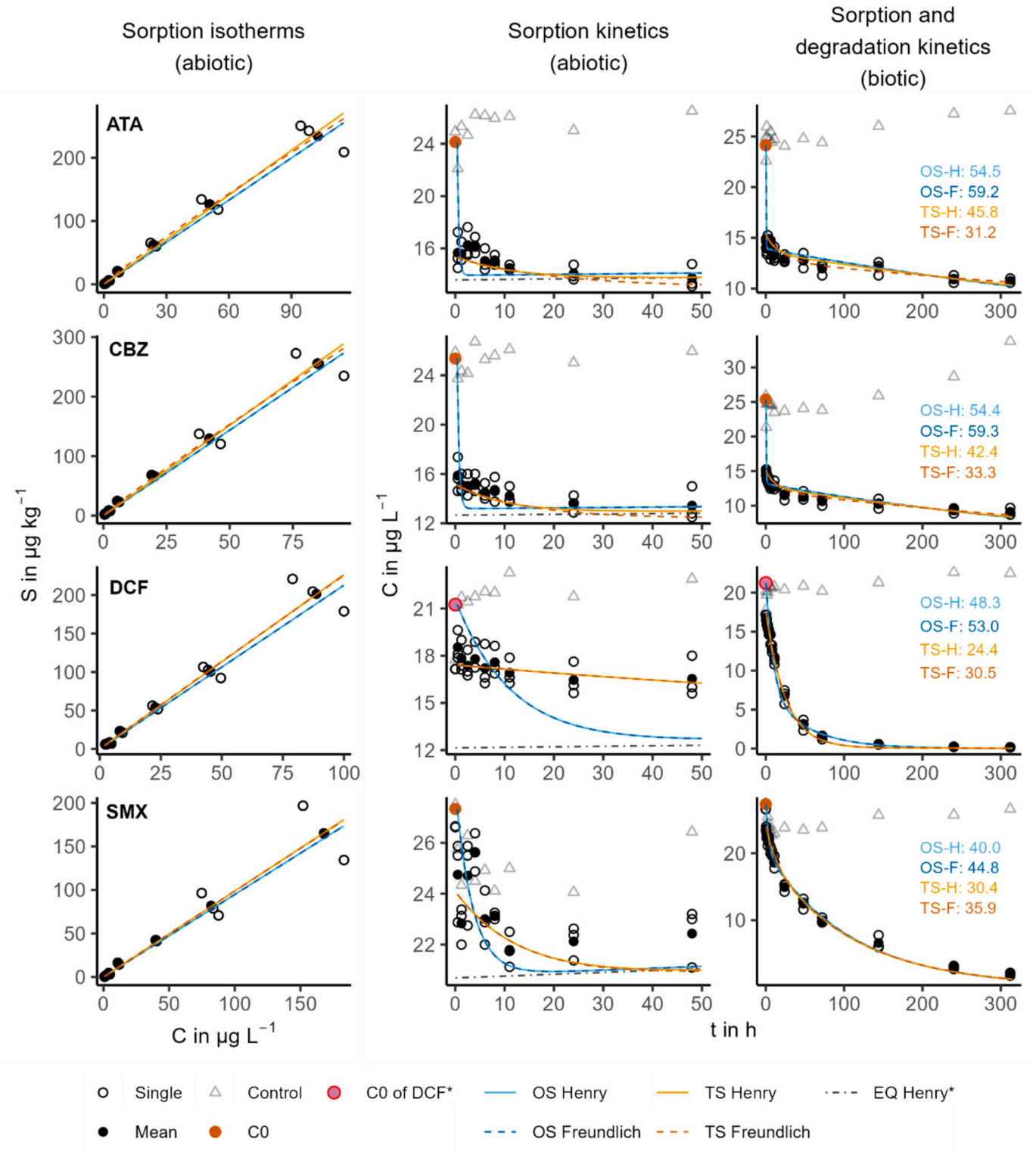

Fig. 2. Measured data and inverse modeling results for simultaneous fitting of the sorption isotherm (first column), sorption kinetics (second column), and coupled sorption and biodegradation kinetics (last column) for ATA, CBZ, DCF and SMX (one per row) using two isotherm models (namely Henry (H) and non-linear Freundlich (F)), and kinetic models (namely one-site (OS) and two-site (TS)). The gray dashed-dotted line in sorption kinetics sub-plots ("EQ Henry*") represent an apparent equilibrium model (only instantaneous sorption), calculated by the linear K_d obtained in isotherm experiment. The colored values in the right subplots are the AIC_C values (lowest AIC_C indicates the most appropriate model).

description of how the biodegradation rates were adjusted to better reflect field conditions is given in the SI (Section S2.2), including Table S1 which summarizes all sorption (isotherm and kinetics), and corrected biodegradation parameters used in the H1D simulations.

4. Results & discussion

4.1. OMP showing sorption and biodegradation

Among the investigated compounds, ATA, CBZ, DCF, and SMX exhibited both sorption and biodegradation (Fig. 2), allowing comprehensive evaluation using the proposed modeling framework (Section 3). For each of these OMP, four distinct model combinations of differing complexity were fitted (Table 5). The colored values in the right subplots are the AIC_C values (lowest AIC_C indicates the most appropriate model; Fig. 2). Fig. 2 also illustrates the fit to the three experimental data types (isotherm, abiotic kinetics, and biotic kinetics), while Table 6 summarizes the corresponding parameters for each fitted model together with the RMSE corresponding to each data type and AIC_C.

According to the lowest AIC_C, the most complex model combining non-linear sorption (Freundlich isotherm) and two-site kinetics described the data for ATA and CBZ best, whereas for DCF and SMX, the linear variant (Henry isotherm) of the two-site kinetics approach was most suitable (Table 6). In general, the sorption was found to be roughly linear as indicated by high Freundlich exponent values $n > 0.93$. This is also reflected by minor differences between model curves for linear and non-linear equilibrium sorption models (Fig. 2, left column).ATA sorption follows a two-sided kinetics, with two thirds of the sorption sites being instantaneously occupied ($f = 0.66$), followed by relatively fast rate-limited sorption ($\alpha = 0.040$ h^{-1}) reaching equilibrium within roughly 12 h. ATA is the only substance, which occurs as cation under the given pH (see Table 2), and therefore likely sorbs to negatively charged soil surface (e.g., dissociated carboxyl or hydroxyl groups) via electrostatic interactions such as cation exchange or electrostatic attraction (Droge and Goss, 2012; Xu et al., 2021). Such sorption mechanisms appear relatively rapid (Strawn, 2021), which supports the findings in this study. According to the estimated K_d and half-live of 12.7 days (Table 6), biodegradation of ATA may be less relevant than sorption in lab-experiments, but will play a crucial role for the fate of ATA under real field-scale transport conditions. However, limited literature data is available for ATA, as ATA has been rarely studied in natural soil matrices.

CBZ sorption showed some similarities to ATA, as it is best described by a two-site kinetic model combined with a non-linear Freundlich isotherm with a fraction of roughly two thirds of instantaneous sorption ($f = 0.627$). Equilibrium for the other sites is roughly reached within 24 h. As a non-ionic and relatively hydrophobic substance (according to its logD of 2.96, Table 2), sorption of CBZ takes place primarily via hydrophobic interactions onto surface groups of organic matter and is therefore strongly correlated with C_{ORG} content in soils (Chefetz et al., 2008; Paz et al., 2016; Kodešová et al., 2015; Filipović et al., 2020). CBZ showed rapid sorption and equilibrium, which is in line with previous studies (Williams et al., 2006; Calisto and Esteves, 2012). Its biodegradation (half-live of 9.6 d) was notably faster than commonly reported in other soil/sediment studies under aerobic conditions, where CBZ is typically persistent (e.g., Yamamoto et al., 2009; Li et al., 2013; Grossberger et al., 2014; Foolad et al., 2015; Martinez-Hernández et al., 2016; Thelusmond et al., 2018). Martinez-Hernández et al. (2016) reported much lower CBZ attenuation in a loamy sand with nearly identical C_{ORG} content in similar approached batch experiments with RW used as liquid phase. Their study, however, only quantified overall removal kinetics without explicitly distinguishing between sorption and microbial degradation, which limits comparability. These deviations may relate to differences in soil organic matter and microbial communities, though these were not characterized in this study.

The data for SMX are best described by a linear sorption isotherm combining a two-site kinetic model. The estimated K_d of 0.99 L kg^{-1} indicates relatively low sorption of SMX onto the examined soil. Under the examined pH (ca. pH 7; Table 3), and according to its pK_a of 5.7 (Table 2), SMX predominantly occurs as anionic species. Accordingly, SMX sorption decreases with increasing pH, as functional groups and SMX dissociate and thereby become more negative enhancing the electrostatic repulsion between sorbent and sorbate (Hu et al., 2019; Wang et al., 2024; Thalmann et al., 2025a, 2025b). Like CBZ, SMX sorption also depends on C_{ORG} content as its sorption is mediated via soil hydrophobic interactions, hydrogen bonds and van der Waals forces (e.

Table 6
Estimated model parameters for ATA, CBZ, DCF, and SMX derived from fitting four different models (see Table 5). For further explanations of the individual parameters refer to Table 4 and Eqs. (1) to (4)). Root mean square errors (RMSE) are reported for each data type: Sorption isotherms ($RMSE_{Iso}$), abiotic kinetics ($RMSE_{abio}$), and biotic degradation kinetics ($RMSE_{bio}$), corresponding with the respective columns of Fig. 2. Boldly marked rows indicate the most suitable model type according to lowest AIC_C value.

OMP	Isotherm	Kinetic model	N_{para} [§]	Parameters						Diagnostic variables			
				Sorption equilibrium		Sorption kinetic		Microbial degradation					
				k_d/k_f	n	α	f	k	DT_{50} [#]	$RMSE_{Iso}$	$RMSE_{abio}$	$RMSE_{bio}$	AIC_C
				L kg^{-1}/ μg^{1-n} L^n kg^{-1}	–	day^{-1}	–	day^{-1}	day	μg kg^{-1}	μg L^{-1}	μg L^{-1}	–
ATA	Henry	One-site	3	2.22	–	45.91	–	0.054	12.7	7.09	3.08	2.85	54.5
	Freund	One-site	4	2.22	1.00*	45.19	–	0.054	12.7	7.06	3.08	2.82	59.2
	Henry	Two-site	4	2.35	–	1.87	0.731	0.050	13.8	4.86	0.66	0.63	45.8
	Freund	**Two-site**	**5**	**3.23**	**0.93**	**0.96**	**0.659**	**0.054**	**12.7**	**1.77**	**0.68**	**0.60**	**31.2**
CBZ	Henry	One-site	3	2.88	–	31.48	–	0.084	8.3	6.64	3.38	3.09	54.4
	Freund	One-site	4	2.88	1.00*	32.63	–	0.084	8.3	6.72	3.38	3.09	59.3
	Henry	Two-site	4	3.04	–	2.09	0.671	0.079	8.8	4.18	0.57	0.67	42.4
	Freund	**Two-site**	**5**	**3.85**	**0.94**	**1.30**	**0.627**	**0.072**	**9.6**	**2.01**	**0.64**	**0.60**	**33.3**
DCF	Henry	One-site	3	2.13	–	1.26	–	1.026	0.7	5.67	2.28	1.96	48.3
	Freund	One-site	4	2.13	1.00*	1.26	–	1.026	0.7	5.67	2.28	1.96	53.0
	Henry	**Two-site**	**4**	**2.27**	**–**	**0.11**	**0.293**	**1.124**	**0.6**	**1.90**	**0.48**	**0.38**	**24.4**
	Freund	Two-site	5	2.37	0.99	0.10	0.288	1.123	0.6	1.88	0.48	0.38	30.5
SMX	Henry	One-site	3	0.95	–	5.24	–	0.308	2.3	3.7	1.81	1.69	40.0
	Freund	One-site	4	0.95	1.00*	5.25	–	0.308	2.3	3.71	1.81	1.69	44.8
	Henry	**Two-site**	**4**	**0.99**	**–**	**1.60**	**0.424**	**0.309**	**2.2**	**1.94**	**1.16**	**0.90**	**30.4**
	Freund	Two-site	5	1.02	0.99	1.55	0.420	0.308	2.3	1.83	1.16	0.90	35.9

[§] N_{para} is the number of fitted parameters
[#] DT_{50} is the half-live value calculated as $DT_{50} = \ln(2)/k$ for better comparability with other findings in literature
* Parameter boundary reached

g. Hu et al., 2019). Park and Huwe (2016) reported comparable K_d values for SMX (0.93–1.48 L kg^{-1}) in a mineral soil with similar properties. Likewise, Mirenga and Thiele-Bruhn (2025) identified biphasic SMX sorption in peat soils consistent with a two-site kinetic model, confirming the sorption dynamics observed in our study. However, sorption capacities in their work were much higher due to the substantially greater C_{ORG} content of peat compared to the loamy sand investigated here, underlining the strong role of C_{ORG} content for SMX sorption. In a similar methodological approach, Martinez-Hernández et al. (2016) observed SMX attenuation in a loamy sand with nearly identical C_{ORG} content, where sorption was comparable to our findings, but overall removal (sorption + biodegradation) was somewhat lower. As with CBZ, their approach quantified only total removal kinetics, without separating sorption from biodegradation, which limits direct comparison. A rapid biodegradation of SMX (estimated half-live of 2.2 days) under aerobic conditions in this study is comparable to findings by Biel-Maeso et al. (2019) in two different soils with similar C_{ORG} content. In another study by Lin and Gan (2011), SMX was transformed under aerobic conditions in two soils with half-live values of 9.4 and 11.4 days. These soils had smaller C_{ORG} contents (both ca. 0.3 %), which may indicate that the degradation of SMX is positively related to the C_{ORG} content.

The fate of DCF cannot be described properly by our modeling approach (Fig. 2). This may result from either very slow sorption kinetics, which seem rather unlikely, or differences in equilibrium sorption behavior between isotherm and abiotic kinetic experiments. This difference could result by variations in experimental boundary conditions or different RW batches. A more detailed discussion is provided in the SI (Section S3.1).

Despite the unsatisfying model fit for DCF, manifesting in likely unrealistically slow sorption kinetics, sorption isotherm and biodegradation data appear reasonably well described (Fig. 2; Table 6). Equilibrium sorption, best represented by a linear Henry model with a K_d of 2.27 L kg^{-1}, is consistent with values reported for similar soils with moderate C_{ORG} (e.g., Revitt et al., 2015; Thalmann et al., 2025a, 2025b). Sorption of DCF is predominantly governed by hydrophobic interactions with C_{ORG}, and limited effects from mineral constituents (Lin and Gan, 2011; Prakathi et al., 2020; De Mastro et al., 2022). Biodegradation of DCF was notably fast, with a half-live of 0.8 days, which is at the lower end of reported values (e.g., Lin and Gan, 2011; Xu et al., 2009), possibly

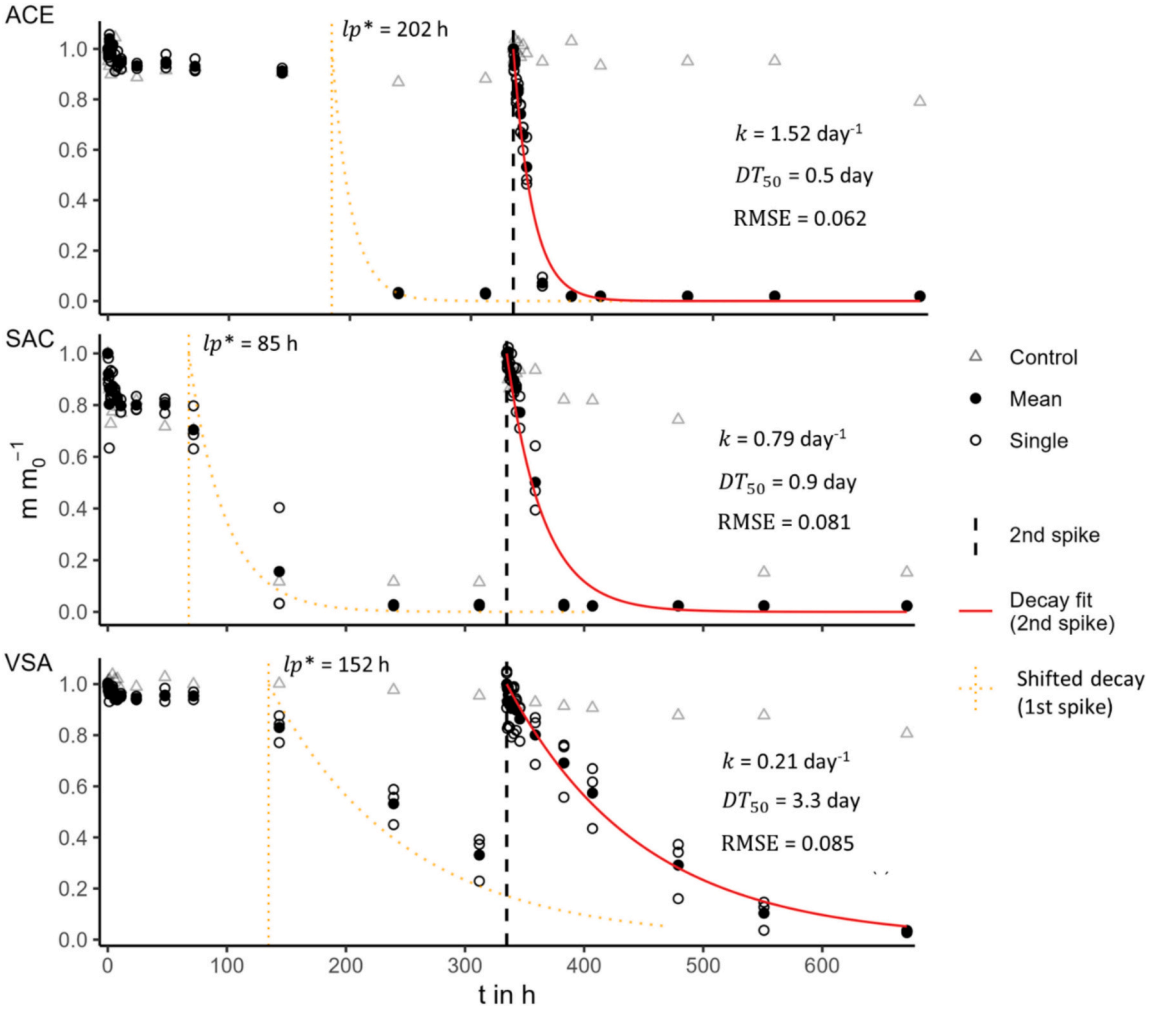

Fig. 3. Relative OMP mass (m m_0, where m is the remaining OMP mass [µg] and m_0 the initial OMP mass [µg]) of ACE, SAC, and VSA in biotic batch experiment following two consecutive OMP spikes. These OMP exhibited negligible sorption and were thus evaluated for biodegradation only. Biodegradation was quantified by fitting a first-order decay model, which accounts for mass increases due to vaporization to the normalized mass data of the second spike (red lines). Fitted degradation rate constant k [day^{-1}], the corresponding half-live [d] ($DT_{50} = ln(2)/k$), and RMSE as a goodness-of-fit metric are reported in each sub-plot. "Control" are control samples (i.e., no soil), "Mean" is the mean value of triplicates, and "Single" are the respective single values of each sample. Lag phase duration (lp*) were estimated by visually aligning the second-spike degradation curve with the first-spike data (orange dotted lines; "Shifted decay"). Notably, initial microbial exposure to OMP began 17 h prior to the first spike due to pre-equilibration with RW, included in lp* values. (For interpretation of the references to colour in this figure legend, the reader is referred to the web version of this article.)

due to enhanced microbial activity in the irrigated topsoil.

4.2. OMP showing solely biodegradation

ACE, SAC, and VSA exhibited negligible sorption to the tested agricultural soil ($K_d < 0.2$ L kg^{-1}), consistent with their high polarity and low logD values (Table 2). Similar findings were observed in previous sorption batch experiments conducted with the same topsoil material under various chemical solution conditions (Thalmann et al., 2025a, 2025b). The dissipation of the three OMP in biotic batch experiments, as shown in Fig. 3 displaying their normalized mass (m/m_0) in biotic batches for two consecutive spikes, could be attributed predominately to biodegradation. Accordingly, the second spike data, reflecting adapted microbial communities, was used for biodegradation rate fitting using a first-order decay model. These models were then shifted on the x-axis to visually estimate lag phases in the first spike, where degradation was initially delayed (lp* in Fig. 3).

ACE and SAC both demonstrated rapid biodegradation after the microbial community had adapted. Half-live values were then 0.5 and 0.9 days for ACE and SAC, respectively (Fig. 3). In contrast, the first spike revealed a delay in degradation, particularly for ACE, where most of the concentration was retained in both controls (without soil) and soil suspensions (with spiked RW) for several days. This suggests that the soil microbiota required an adaptation phase before ACE degradation initiated. For SAC, an initial decline was observed even in the controls (no soil), implying that a portion of its biodegradation was mediated by microbes already present in the RW (indicating microbial activity although it was UV-treated). However, a stronger degradation response emerged in soil suspensions in the sample taken after 240 h, which may indicate a microbial adaptation of the soil community, consistent to the lag phase for ACE degradation.

Literature on the biodegradability of ACE and SAC in soils reflects similar patterns as observed in our experiments. While ACE has been considered persistent in aquatic systems (e.g., Belton et al., 2020) or during riverbank filtration (Scheurer et al., 2011; Jekel et al., 2015; Storck et al., 2016), implying its persistence in theses systems, recent studies have reported its biodegradability in aerobic degradation experiments conducted with different natural soils. Biel-Maeso et al. (2019), for instance, observed half-lives of 11 to 19 days for ACE and roughly 5 days for SAC in two agricultural soils in batch systems, with reported lag phases of about 4 days. Furthermore, Burke et al. (2018) reported half-lives (normalized values to soil moisture at field capacity) between 1.5 and 27 days for ACE and 1.6 to 8.2 days for SAC, for different agricultural soils. These studies indicate that microbial adaptation and soil properties such as organic carbon content can significantly affect degradation rates. In the present study, the notably faster dissipation of ACE and SAC may be favored by the relatively high C_{ORG} and, importantly, to the 17-h pre-equilibration with RW prior to first OMP spike (see Section 0).

Valsartanate (VSA) also showed a pattern of delayed but significant biodegradation, similar to ACE and SAC (Fig. 3). No removal occurred during the initial lag phase in the first spike, but following microbial adaptation, VSA was degraded with a half-live of 3.3 days. Similar to ACE, degradation was absent in control samples, supporting the interpretation that microbial transformation was exclusively mediated by the indigenous soil microbiota. Findings on the environmental fate of VSA in soils are sparse. However, our results roughly align with those from column studies simulating bank filtration conducted by Burke et al. (2018), who observed that VSA is degraded very quickly (half-live of 0.5 h) under warm, oxic sediment conditions.

The observed lag phases across all three OMP highlight the importance of microbial acclimation in soil systems and the need to consider these adaption periods in biodegradation studies by extending the experiment with a second spike event.

The remaining three substances DZA, TFMSA, and PRI exhibited no or not quantifiable low reactivity in all experiments, indicating mobile and persistent behaviors of these OMP in the tested soil under the experimental conditions. A detailed discussion is given in the SI in section S3.2.

4.3. Implications in field simulations

The relevance of lab-derived sorption kinetics parameters for predicted field-scale transport of ATA, CBZ, DCF, and SMX was evaluated through comparative simulations using Hydrus-1D, distinguishing rate-limited sorption ("Non-EQ", Fig. 4) versus instantaneous equilibrium assumptions ("EQ", Fig. 4). Across a three-year simulation period after RW irrigation initiated, both approaches yielded nearly identical OMP fluxes at 10, 20, and 30 cm depths.

Additionally, these results were robust across contrasting hydrologic settings. Varying both climate (humid vs. semi-arid) and lower boundary conditions (deep groundwater, free drainage, vs. shallow groundwater, constant head h = 0 cm) produced only marginal changes in the relative differences between non-equilibrium and equilibrium sorption simulations at 10–30 cm (Fig. A2). These additional simulations indicate that our base-case finding is insensitive to climatic forcing and lower groundwater conditions under matrix-dominated flow.

This result indicates that despite evident rate-limited sorption observed in batch experiments, incorporating sorption kinetics in simulations of field OMP transport did not have a significant effect, and this holds across semi-arid/humid climates and deep/shallow groundwater conditions. This is not surprising for ATA, CBZ, and SMX, for which equilibrium was roughly reached within 24 h in the laboratory experiments (Fig. 2). DCF presents an extreme scenario with likely unrealistically slow sorption ($\alpha = 0.11$ day^{-1}, Table 6) due to discrepancies in sorption between isotherm and kinetic batch experiments as discussed above. Despite this unrealistically slow sorption, the non-equilibrium simulation yielded only marginally increased cumulative DCF fluxes compared to the equilibrium scenario (Fig. 4), suggesting a limited effect on OMP transport under typical model assumptions.

The limited impact of sorption kinetics on field-scale transport in our simulations aligns with findings by de Wilde et al. (2008), who showed that sorption kinetics mainly affect solute leaching when the residence time in the soil is short. Rahman et al. (2004) similarly emphasized the importance of sorption kinetics under preferential flow, where rapid solute movement limits sorption equilibrium adjustment in soils. Radolinski et al. (2022) demonstrated that the degree of preferential flow critically governs the relevance of non-equilibrium assumptions, while Maraqa and Khashan (2014) confirmed that kinetic effects diminish under uniform flow but are significant in systems with fast solute transport and heterogeneous sorption sites.

To evaluate the relevance of microbial adaptation time for field-scale transport, H1D simulations were conducted for ACE, SAC, and VSA with and without inclusion of the experimentally observed lag phases (Fig. 5). Across all three OMP, cumulative fluxes at 10, 20, and 30 cm depths were nearly identical between both simulation scenarios. Only ACE, which exhibited the longest lag phase (9 d), showed a marginal increase in solute flux at 10 cm depth when lagged degradation was considered. However, this difference became negligible at greater depths, indicating minimal influence of microbial lag phases on overall transport under the simulated conditions.

The sensitivity analysis across climate and groundwater conditions likewise to sorption kinetics showed minor effects of microbial adaptation time on near-surface fluxes (Fig. A3). In all cases, effects diminished with depth and did not alter domain-integrated observations. Hence, the lag/no-lag contrast is largely insensitive to the tested climatic forcing and lower-boundary conditions under matrix-dominated flow.

Nevertheless, under fast transport conditions and/or prolonged lag phases, microbial degradation may be delayed, allowing OMP to bypass reactive topsoil layers before biodegradation begins, thereby increasing the risk of groundwater contamination. Microbial adaptation to xenobiotics has been shown to require up to several weeks in previously

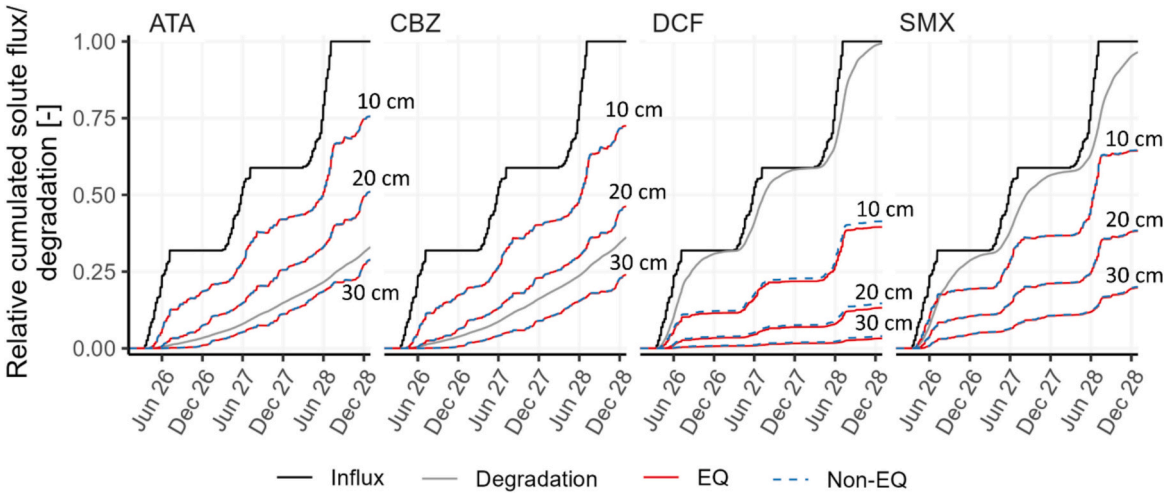

Fig. 4. Simulation results of ATA, CBZ, DCF, and SMX three years after irrigation start showing the relative cumulated solute fluxes at 0 (influx), 10, 20, and 30 cm depth one considering rate-limited sorption (Non-EQ) and another assuming instantaneous equilibrium sorption (EQ). Relative cumulative solute flux and degradation (cumulative value of entire soil domain) were calculated by normalizing to the total solute influx relative to the maximum influx at last time t_{max}. All reaction parameters used in H1D are summarized in Table S1.

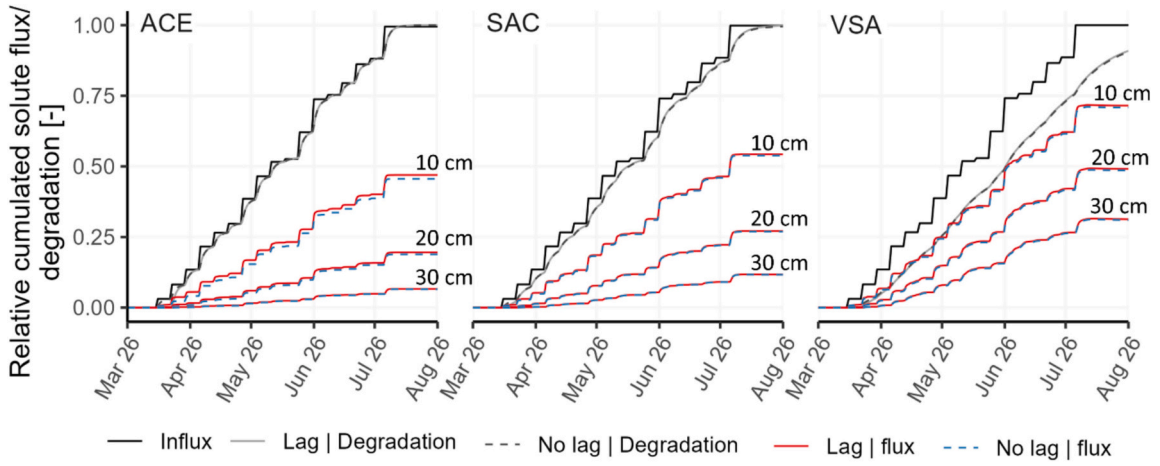

Fig. 5. Simulated relative cumulative solute fluxes and microbial degradation of ACE, SAC, and VSA at 10, 20, and 30 cm depths during the first irrigation season after the onset of irrigation with reclaimed water (RW). Simulations compare scenarios with experimentally observed microbial lag phases (solid red lines: "Lag") to those without lag phases (dashed blue lines: "No lag"), where degradation initiates immediately upon OMP entry into the soil. The gray lines indicate cumulative microbial degradation, and the black line represents the total solute influx at the soil surface (0 cm). All values are normalized to total influx at t_{max}. Parameter values used for degradation and lag phases are summarized in Table S1. (For interpretation of the references to colour in this figure legend, the reader is referred to the web version of this article.)

unexposed soils (Dechesne et al., 2014; de Wilt et al., 2018). If such adaptation delays coincide with rapid leaching (e.g., in coarsely textured or soils that are dominated by preferential flow) OMP may be transported beyond the predominantly biological active zones before degradation can occur (Sandrin et al., 2001; Bertelkamp et al., 2015).

Taken together, these findings indicate that while sorption kinetics and microbial adaptation should be considered when deriving parameters from lab-scale data, they have limited effect on simulation results representing field-scale transport under matrix-dominated conditions. Simplified assumptions (i.e., instantaneous sorption and immediate biodegradation) provided similar predictions to more complex simulations. Thus, for homogeneous soils irrigated with RW, such simplifications are justified and can support site-specific risk assessments using established tools like FOCUS PELMO (FOCUS, 2021), FOCUS PEARL (Leistra et al., 2001), or Hydrus-1D (Šimůnek et al., 2013). However, under conditions promoting short residence times or delayed microbial adaptation, neglecting these processes may underestimate OMP mobility and related risks.

4.4. Study limitations

This study presents a comprehensive integrative approach that combines batch experiment findings with advanced data modeling to support field-scale simulations assessing the fate of OMP in soils under reclaimed water irrigation. However, some limitations are acknowledged in the following:

- The use of NaN_3 (0.2 g L^{-1}) to inhibit microbial activity in abiotic batch experiments may introduce uncertainty, as its sterilization efficiency depends on concentration, exposure duration, and the native microbial community (Lees et al., 2018; Otte et al., 2018; Süßmuth et al., 2024). While degradation was likely suppressed during the period of 48 h considered for sorption equilibrium, NaN_3 may alter soil properties (Trevors, 1996) or react with certain

analytes (Chafetz et al., 2006), potentially affecting sorption dynamics. These effects were evaluated via control batches and concomitant parameter monitoring (see SI, Section S1.2).

- The modeling approach assumes fully reversible, non-hysteretic sorption, which may oversimplify actual OMP-soil interactions, and was found to be relevant for various OMP (e.g., reviewed by Alhalabi et al., 2024).
- Biodegradation rates used in the H1D simulations were corrected for field-relevant factors such as soil depth, temperature, and moisture (detailed in SI; Section S1.3). However, these rates remained static and did not account for temporal variability in microbial activity and environmental conditions, due to seasonal shifts or short-term environmental fluctuations, potentially limiting the accuracy of long-term predictions.
- H1D simulations assume uniform matrix flow, excluding preferential flow and transport heterogeneities. This may underestimate the impacts of sorption kinetics and lag phase on OMP transport, i.e., in structured soils which are affected by preferential flow and rapid transport dynamics.

Despite these limitations, the study offers robust insights into the dominant processes of OMP fate and their importance for field-scale transport modeling, supporting simplified modeling assumptions under defined conditions as is usually the case for typical risk assessment tools such as FOCUS PELMO, FOCUS PEARL, and H1D. While the field simulations provide scenario-based predictions, to evaluate the theoretical relevance of these dynamic factors of lab-driven parameters these scenarios do not substitute for empirical validation under actual field conditions.

5. Summary & conclusion

This study presents an integrative approach combining findings from batch experiments with advanced modeling and process-based field-scale simulations to investigate the environmental fate of ten OMP in an agricultural topsoil in context of irrigation with RW. Parameters for sorption isotherms, sorption kinetics, and microbial degradation were estimated from laboratory data using a robust inverse modeling framework, which simultaneously fitted multiple data types and explicitly accounted for vaporization from aerated batch vessels.

ATA, CBZ, and SMX exhibited biphasic sorption behavior, with a rapid initial phase followed by a slower approach to equilibrium within 24 h. A two-site kinetic model provided the best fit based on the lowest AIC_C values. Notably, CBZ exhibited faster degradation than typically reported, suggesting that site-specific microbial adaptation and soil organic matter may significantly alter degradation dynamics. Six OMP (ACE, SAC, VSA, DZA, PRI, TFMSA) exhibited negligible sorption, whereas of these DZA, PRI, TFMSA were also not biodegraded, indicating their mobility and persistence under the experimental conditions. In contrast, ACE, SAC, and VSA, following lag phases between 4 and 9 days, were biodegraded relatively rapidly with half-lives of 0.4, 0.9, and 3.3 days, respectively.

Field-scale simulations using Hydrus-1D assessed the relevance of sorption kinetics and microbial lag phases under typically assumed site conditions for model-based risk assessment. While these dynamic factors were essential for a correct parameterization at the laboratory scale, simulations showed negligible impacts on field-scale transport of OMP under matrix-dominated flow conditions. These findings imply that, especially in homogeneous soils, simplified simulation approaches assuming instantaneous sorption and immediate biodegradation may be sufficient for reliable model-based risk assessment. However, when OMP exhibit slow sorption or prolonged lag phases, particularly in soils with rapid water and OMP transport, such as coarsely-textured or soils dominated by preferential flow, these processes may significantly affect transport of OMP and should be explicitly considered. While our findings support simplified model assumptions under contrasting climates and groundwater conditions (deep vs. shallow) in the studied loamy sand, further work on other soils with different reactivity is needed to test whether these conclusions are transferable.

Ultimately, this study provides a comprehensive framework for linking lab-scale parameterization with field-scale simulations to assess the fate of OMP in agriculture irrigated with RW. These insights can help streamline regulatory groundwater risk assessments by supporting the use of simplified transport models under well-characterized, soil matrix-dominated conditions, thereby improving efficiency without compromising scientific robustness. Future research should focus on empirical validation of sorption kinetics and microbial adaptation periods under realistic field conditions, particularly targeting scenarios involving preferential flow or limited microbial pre-exposure, to robustly quantify transport risks.

CRediT authorship contribution statement

Mogens Thalmann: Writing – review & editing, Writing – original draft, Visualization, Methodology, Investigation, Formal analysis, Data curation, Conceptualization. **Sondra Klitzke:** Writing – review & editing, Conceptualization. **Andrea Lange:** Writing – review & editing, Methodology, Formal analysis. **Aki Sebastian Ruhl:** Writing – review & editing, Project administration. **Andre Peters:** Writing – review & editing, Supervision, Methodology, Formal analysis, Conceptualization.

Declaration of generative AI and AI-assisted technologies in the writing process

During the preparation of this work the authors used ChatGPT (OpenAI; model GPT-4o) in order to **improve the clarity and linguistic quality of the manuscript**. After using this tool, the authors reviewed and edited the content as needed and take full responsibility for the content of the published article.

Funding

This work was supported by the German Federal Ministry of Education and Research (BMBF, Bonn) through the project “Point-of-Use Re-Use: Dezentrale landwirtschaftliche Wiederverwendung von häuslichem Abwasser zur Verringerung von Nutzungskonkurrenzen” – PU_2R (FKZ: 02WV1564H). Open Access funding enabled and organized by Project DEAL.

Declaration of competing interest

The authors declare that they have no known competing financial interests or personal relationships that could have appeared to influence the work reported in this paper.

Acknowledgements

The authors thank Friedrich Trepte for his valuable support in conducting kinetic batch experiments and preparing samples for HPLC-MS/MS analysis. We kindly thank Silke Pabst for HPLC-MS/MS analysis. We are also grateful to Birgit Walter for performing the soil characterizations at TU Braunschweig. Moreover, thanks go to Daniel Dittmann and Sascha Iden for insightful discussions and input during the early conceptual stages of this study.

Appendix A. Appendix

A.1. Derivation of governing equation system

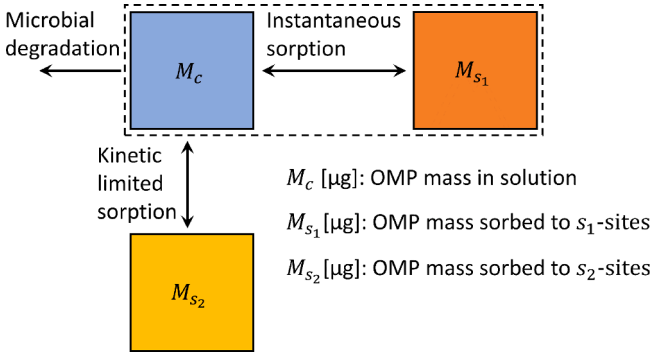

Fig. A1. Compartment model for OMP fate in batch experiments with mass balance approach.

The mathematical derivation of the most complex equation system (i.e., Freundlich isotherm and two-site kinetic sorption model) incorporating the changing soil-solution-ratio according to a zero-order vaporization of water is described as follows with some general definitions to begin with:

$$M_c = Vc \tag{A1}$$

where M_c [µg] is the mass of the OMP in solution, V [L] is the solution volume and c [µg L^{-1}] is the OMP solution concentration.

$$M_s = M_{s_1} + M_{s_2} \tag{A2}$$

where M_s [µg], is the total sorbed OMP mass as sum of OMP mass sorbed to s_1 and s_2 sites (M_{s_1} and M_{s_2}).

$$s = \frac{M_s}{m} = s_1 + s_2 \tag{A3}$$

where s [µg kg^{-1}] is the total sorbed concentration at both types of sorption sites, m [kg] is the soil mass in the batch, s_1 [µg kg^{-1}] is the sorbed concentration at s_1-sites (instantaneous equilibrium), and s_2 [µg kg^{-1}] is the sorbed concentration at s_2-sites (kinetically limited).

At equilibrium, the s_1 and s_2 are defined as:

$$s_{1,eq} = s_1 = f\, s_{eq} \tag{A4}$$

$$s_{2,eq} = (1-f)\, s_{eq} \tag{A5}$$

where f [−] is the fraction of s_1-sites, and s_{eq} [µg kg^{-1}] is the sorbed concentration after equilibrium adjustment defined by the Freundlich isotherm for the most complex case:

$$s_{eq}(c) = k_f c^n \tag{A6}$$

with k_f [$\mu g^{1\text{-}n}\, L^n\, kg^{-1}$] is the Freundlich distribution coefficient, n [−] is the Freundlich exponent (restrained to values ≤1, as higher values lead to isotherms which are mechanistically not plausible).

Because batch flasks where shaken open to allow aeration during the experiment, solution volume changes linear described by a zero-order model:

$$\frac{dV}{dt} = -\gamma \tag{A7}$$

where γ [L h^{-1}] is the vaporization rate constant.

The mass changes in solution plus sorbed to s_1-sites (area within dashed line in Fig. A1), and the mass sorbed to s_2-sites can be defined as:

$$\frac{dM_c}{dt} + \frac{dM_{s_1}}{dt} = -kM_c - m\alpha\left[(1-f)s_{eq}(c) - s_2\right] \tag{A8}$$

$$\frac{dM_{s_2}}{dt} = m\alpha\left[(1-f)s_{eq}(c) - s_2\right] \tag{A9}$$

where k [h^{-1}] is the is the first-order rate constant for microbial degradation, and α [h^{-1}] is the rate constant for kinetically limited sorption (s_2-sites). The first term on the right side of Eq. (A8) describes the first order degradation and the second the "loss" towards the s_2-sites.

As $M_{s_2} = ms_2$, and m is constant, Eq. (A9) simplifies to (equaling Eq. (4)):

$$\frac{ds_2}{dt} = \alpha\left[(1-f)s_{eq}(c) - s_2\right] \tag{A10}$$

Using Eq. (A1) and $M_{s1} = mfs_{eq}$, Eq. (A8) becomes:

$$\frac{dVc}{dt} + mf\frac{ds_{eq}}{dt} = -kVc - m\alpha\left[(1-f)s_{eq}(c) - s_2\right] \tag{A11}$$

Then, using the product rule in $\frac{dVc}{dt}$ and chain rule in second term $\frac{ds_{eq}}{dt}$, we get:

$$c\frac{dV}{dt} + V\frac{dc}{dt} + mf\frac{ds_{eq}}{dc}\frac{dc}{dt} = -kVc - m\alpha\left[(1-f)s_{eq}(c) - s_2\right] \tag{A12}$$

Using Eq. (A7) in Eq. (A12) brings:

$$-c\gamma + \left(V + mf\frac{ds_{eq}(c)}{dc}\right)\frac{dc}{dt} = -kVc - m\alpha\left[(1-f)s_{eq}(c) - s_2\right] \tag{A13}$$

Rearranged Eq. (A13) for $\frac{dc}{dt}$ (yields)

$$\frac{dc}{dt} = -\frac{(kV-\gamma)c + m\alpha\left[(1-f)s_{eq}(c) - s_2\right]}{V + mf\frac{ds_{eq}(c)}{dc}} \tag{A14}$$

Using the first derivation of the Freundlich isotherm (Eq. (A6)) in Eq. (A14) yields the final differential equation for the time-dependent concentration identical to Eq. (3):

$$\frac{dc}{dt} = -\frac{(kV-\gamma)c + m\alpha\left[(1-f)k_f c^n - s_2\right]}{V + mfnk_f c^{n-1}} \tag{A15}$$

Summarizing, the 4 coupled differential equations are:

$$\frac{dV}{dt} = -\gamma \tag{A16}$$

$$s_{eq}(c) = k_f c^n \tag{A17}$$

$$\frac{dc}{dt} = -\frac{(kV-\gamma)\,c + m\alpha\left[(1-f)\,s_{eq}(c) - s_2\right]}{V + mfs_{eq}(c)'} \tag{A18}$$

$$\frac{ds_2}{dt} = \alpha\left[(1-f)\,s_{eq}(c) - s_2\right] \tag{A19}$$

A.2. Field-scale sensitivity of kinetic vs. instantaneous sorption to hydrologic setting

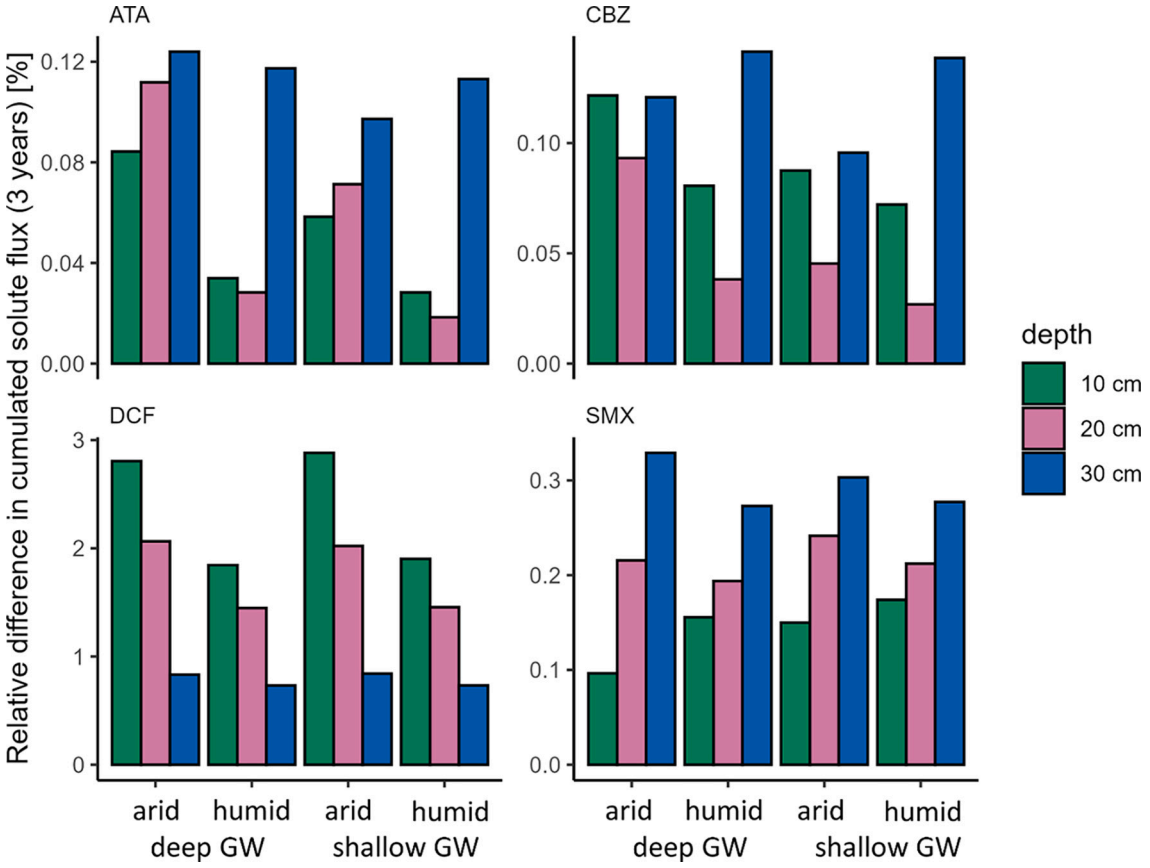

Fig. A2. Sensitivity of the sorption-kinetics effect to climate and groundwater proximity at field scale. Bars show the relative difference (%) in cumulative solute flux over 3 years between non-equilibrium (first-order kinetic) and instantaneous sorption simulations at 10, 20, and 30 cm for ATA, CBZ, DCF, and SMX. Scenarios span humid vs. semi-arid (just arid in figure for brevity) climate forcing and two lower boundary conditions: free drainage (deep groundwater) and constant pressure head h = 0 cm at the lower boundary (shallow groundwater). All other inputs match the base configuration. GW abbreviates groundwater.

A.2.1. Field-scale sensitivity of lag vs. no-lag degradation to hydrologic setting

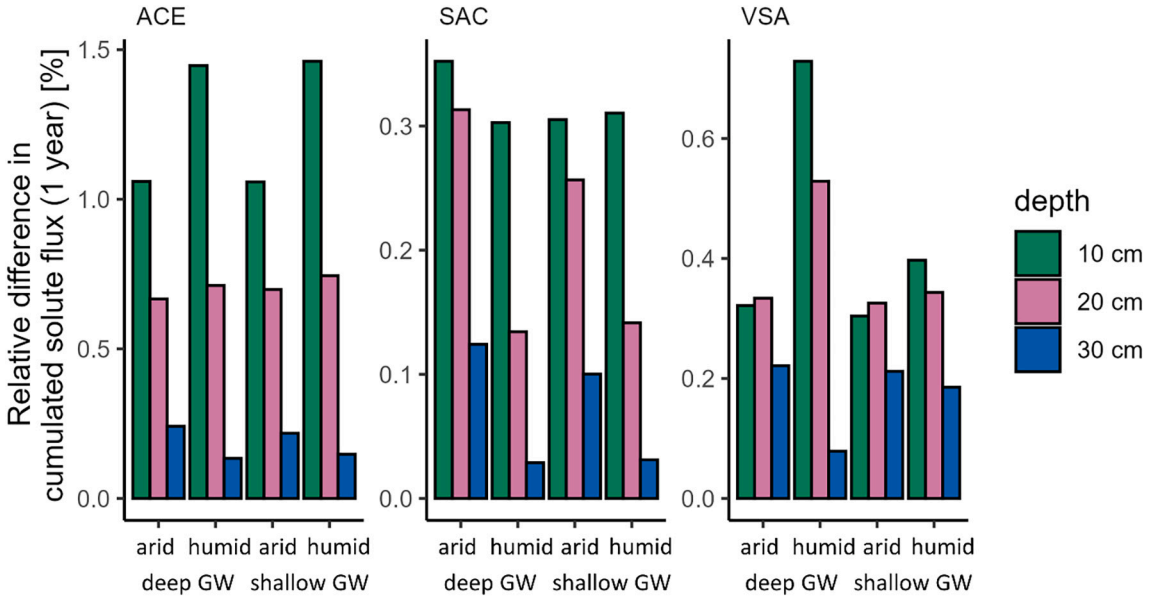

Fig. A3. Sensitivity of the lag-phase effect to climate and groundwater proximity at field scale. Bars show the relative difference (%) in cumulative solute flux over 1 year between simulations with measured microbial lag phases and without lag at 10, 20, and 30 cm for ACE, SAC, and VSA. Scenarios span humid vs. semi-arid (just arid in figure for brevity) climate forcing and two lower boundary conditions: free drainage (deep groundwater) and constant pressure head h = 0 cm at the lower boundary (shallow groundwater). All other inputs match the base configuration. GW abbreviates groundwater.

Appendix B. Supplementary data

Supplementary data to this article can be found online at https://doi.org/10.1016/j.jconhyd.2025.104779.

Data availability

The data that the extensive H1D simulations are based on is going to be made available upon request after acceptance of our manuscript.

References

Abdallat, G.A., Salameh, E., Shteiwi, M., Bardaweel, S., 2022. Pharmaceuticals as Emerging Pollutants in the Reclaimed Wastewater Used in Irrigation and Their Effects on Plants, Soils, and Groundwater. Water 14, 1560. https://doi.org/10.3390/w14101560.

Alhalabi, A.M., Meetani, M.A., Shabib, A., Maraqa, M.A., 2024. Sorption of pharmaceutically active compounds to soils: a review. Environ. Sci. Eur. 36. https://doi.org/10.1186/s12302-024-00984-9.

Ali, M.Z., Ishak, K.M., Zawawi, M.A., Jaafar, M., Ahmad, Z., 2022. Simultaneous enhancement of conductivity and Seebeck coefficient of PEDOT:PSS by triflic acid treatment for flexible thermoelectric generator. Synth. Met. 286, 117037. https://doi.org/10.1016/j.synthmet.2022.117037.

Banzhaf, S., Hebig, K.H., 2016. Use of column experiments to investigate the fate of organic micropollutants – a review. https://doi.org/10.5194/hess-2016-196.

Avisar, D., Lester, Y., Ronen, D., 2009. Sulfamethoxazole contamination of a deep phreatic aquifer. Sci. Total Environ. 407 (14), 4278–4282. https://doi.org/10.1016/j.scitotenv.2009.03.032.

Barra Caracciolo, A., Topp, E., Grenni, P., 2015. Pharmaceuticals in the environment: Biodegradation and effects on natural microbial communities. A review. J. Pharm. Biomed. Anal. 106, 25–36. https://doi.org/10.1016/j.jpba.2014.11.040.

Belete, B., Desye, B., Ambelu, A., Yenew, C., 2023. Micropollutant Removal Efficiency of Advanced Wastewater Treatment Plants: A Systematic Review. Environmental Health Insights 17. https://doi.org/10.1177/11786302231195158.

Belton, K., Schaefer, E., Guiney, P.D., 2020. A Review of the Environmental Fate and Effects of Acesulfame-Potassium. Integr. Environ. Assess. Manag. 16, 421–437. https://doi.org/10.1002/ieam.4248.

Bertelkamp, C., Schoutteten, K., Vanhaecke, L., Vanden Bussche, J., Callewaert, C., Boon, N., Verliefde, A.R., 2015. A laboratory-scale column study comparing organic micropollutant removal and microbial diversity for two soil types. Sci. Total Environ. 536, 632–638. https://doi.org/10.1016/j.scitotenv.2015.07.056.

Biel-Maeso, M., González-González, C., Lara-Martín, P.A., Corada-Fernández, C., 2019. Sorption and degradation of contaminants of emerging concern in soils under aerobic and anaerobic conditions. Sci. Total Environ. 666, 662–671. https://doi.org/10.1016/j.scitotenv.2019.02.279.

Bijlsma, L., Pitarch, E., Fonseca, E., Ibáñez, M., Botero, A.M., Claros, J., Hernández, F., 2021. Investigation of pharmaceuticals in a conventional wastewater treatment plant: Removal efficiency, seasonal variation and impact of a nearby hospital. Journal of Environmental Chemical Engineering 9, 105548. https://doi.org/10.1016/j.jece.2021.105548.

Branco, R.H., Meulepas, R.J., Van Veelen, Rijnaarts, H.H., Sutton, N.B., 2023. Influence of redox condition and inoculum on micropollutant biodegradation by soil and activated sludge communities. Sci. Total Environ. 897, 165233. https://doi.org/10.1016/j.scitotenv.2023.165233.

Buerge, I.J., Keller, M., Buser, H.-R., Müller, M.D., Poiger, T., 2010. Saccharin and Other Artificial Sweeteners in Soils: Estimated Inputs from Agriculture and Households, Degradation, and Leaching to Groundwater. Environ. Sci. Technol. 45, 615–621. https://doi.org/10.1021/es1031272.

Burke, V., Schneider, L., Greskowiak, J., Zerball-van Baar, P., Sperlich, A., Dünnbier, U., Massmann, G., November 2018. Trace Organic Removal during River Bank Filtration for Two Types of Sediment. Water 10, 1736. https://doi.org/10.3390/w10121736.

Calisto, V., Esteves, V.I., 2012. Adsorption of the antiepileptic carbamazepine onto agricultural soils. J. Environ. Monit. 14, 1597. https://doi.org/10.1039/c2em10895j.

Campan, P., Samouelian, A., Voltz, M., 2023. Evaluation of temperature corrections for pesticide half-lives in tropical and temperate soils. Environ. Sci. Pollut. Res. 30 (21468–21), 480. https://doi.org/10.1007/s11356-022-23,566-9.

Chefetz, B., Mualem, T., Ben-Ari, J., 2008. Sorption and mobility of pharmaceutical compounds in soil irrigated with reclaimed wastewater. Chemosphere 73, 1335–1343. https://doi.org/10.1016/j.chemosphere.2008.06.070.

Chemaxon, 2025. Chemicalize. Version Radium 25 (1), 2. Retrieved from https://chemicalize.com.

Chorover, J., Brusseau, M.L., 2008. Kinetics of Sorption—Desorption. In: Kinetics of Water-Rock Interaction. Springer, New York, pp. 109–149. https://doi.org/10.1007/978-0-387-73,563-4_4.

De Mastro, F., Cacace, C., Traversa, A., Pallara, M., Cocozza, C., Mottola, F., Brunetti, G., 2022. Influence of chemical and mineralogical soil properties on the adsorption of sulfamethoxazole and diclofenac in Mediterranean soils. Chem. Biol. Technol. Agric. 9. https://doi.org/10.1186/s40538-022-00300-8.

de Wilde, T., Mertens, J., Spanoghe, P., Ryckeboer, J., Jaeken, P., Springael, D., 2008. Sorption kinetics and its effects on retention and leaching. Chemosphere 72, 509–516. https://doi.org/10.1016/j.chemosphere.2008.02.053.

de Wilt, A., He, Y., Sutton, N., Langenhoff, A., Rijnaarts, H., 2018. Sorption and biodegradation of six pharmaceutically active compounds under four different redox conditions. Chemosphere 193, 811–819. https://doi.org/10.1016/j.chemosphere.2017.11.084.

Dechesne, A., Badawi, N., Aamand, J., Smets, B.F., 2014. Fine scale spatial variability of microbial pesticide degradation in soil: scales, controlling factors, and implications. Front. Microbiol. 5. https://doi.org/10.3389/fmicb.2014.00667.

Droge, S., Goss, K.-U., 2012. Effect of Sodium and Calcium Cations on the Ion-Exchange Affinity of Organic Cations for Soil Organic Matter. Environ. Sci. Technol. 46, 5894–5901. https://doi.org/10.1021/es204449r.

Durner, W., Iden, S.C., 2021. The improved integral suspension pressure method (ISP+) for precise particle size analysis of soil and sedimentary materials. Soil Tillage Res. 213, 105086. https://doi.org/10.1016/j.still.2021.105086.

Feifel, M., Durner, W., Hohenbrink, T.L., Peters, A., 2024. Effects of improved water retention by increased soil organic matter on the water balance of arable soils: A numerical analysis. Vadose Zone J. 23. https://doi.org/10.1002/vzj2.20302.

Filipović, L., Filipović, V., Walker, C.W., Williams, C., Preisdanz, H.E., Watson, J.E., 2020. Modeling carbamazepine transport in wastewater-irrigated soil under different land uses. J. Environ. Qual. 49, 1011–1019. https://doi.org/10.1002/jeq2.20074^.

FOCUS, 2021. Generic Guidance for Tier 1 FOCUS Ground Water Assessments. Version 2.3. retrived from. https://esdac.jrc.ec.europa.eu/public_path/projects_data/focus/gw/docs/Generic_guidance_FOCUS_GW_V2-3final.pdf.

Foolad, M., Hu, J., Tran, N.H., Ong, S.L., 2015. Sorption and biodegradation characteristics of the selected pharmaceuticals and personal care products onto tropical soil. Water Sci. Technol. 73, 51–59. https://doi.org/10.2166/wst.2015.461.

Ghosh, G.C., Nakada, N., Yamashita, N., Tanaka, H., 2010. Occurrence and fate of oseltamivir carboxylate (Tamiflu) and amantadine in sewage treatment plants. Chemosphere 81, 13–17. https://doi.org/10.1016/j.chemosphere.2010.07.023.

Gibson, R., Durán-Álvarez, J.C., Estrada, K.L., Chávez, A., Cisneros, B.J., 2010. Accumulation and leaching potential of some pharmaceuticals and potential endocrine disruptors in soils irrigated with wastewater in the Tula Valley, Mexico. Chemosphere 81 (11), 1437–1445. https://doi.org/10.1016/j.chemosphere.2010.09.006.

Greskowiak, J., Hamann, E., Burke, V., Massmann, G., 2017. The uncertainty of biodegradation rate constants of emerging organic compounds in soil and groundwater – A compilation of literature values for 82 substances. Water Res. 126, 122–133. https://doi.org/10.1016/j.watres.2017.09.017.

Grossberger, A., Hadar, Y., Borch, T., Chefetz, B., 2014. Biodegradability of pharmaceutical compounds in agricultural soils irrigated with treated wastewater. Environ. Pollut. 185, 168–177. https://doi.org/10.1016/j.envpol.2013.10.038.

Gworek, B., Kijeńska, M., Wrzosek, J., Graniewska, M., 2021. Pharmaceuticals in the Soil and Plant Environment: a Review. Water Air Soil Pollut. 232. https://doi.org/10.1007/s11270-020-04954-8.

Hashem, M.S., Qi, X., 2021. Treated wastewater irrigation—A review. Water 13 (11), 1527. https://doi.org/10.3390/w13111527.

Heistermann, M., Jene, B., Fent, G., Feyerabend, M., Seppelt, R., Richter, O., Kubiak, R., 2003. Modeling approaches to compare sorption and degradation of metsulfuron-methyl in laboratory micro-lysimeter and batch experiments. Pest Manag. Sci. 59, 1276–1290. https://doi.org/10.1002/ps.765.

Helmecke, M., Fries, E., Schulte, C., 2020. Regulating water reuse for agricultural irrigation: risks related to organic micro-contaminants. Environ. Sci. Eur. 32. https://doi.org/10.1186/s12302-019-0283-0.

Hu, S., Zhang, Y., Shen, G., Zhang, H., Yuan, Z., Zhang, W., 2019. Adsorption/desorption behavior and mechanisms of sulfadiazine and sulfamethoxazole in agricultural soil systems. Soil Tillage Res. 186, 233–241. https://doi.org/10.1016/j.still.2018.10.026.

Huntscha, S., Singer, H.P., McArdell, C.S., Frank, C.E., Hollender, J., 2012. Multiresidue analysis of 88 polar organic micropollutants in ground, surface and wastewater using online mixed-bed multilayer solid-phase extraction coupled to high performance liquid chromatography–tandem mass spectrometry. J. Chromatogr. A 1268, 74–83. https://doi.org/10.1016/j.chroma.2012.10.032.

Hurtado, C., Montano-Chávez, Y.N., Domínguez, C., Bayona, J.M., 2017. Degradation of Emerging Organic Contaminants in an Agricultural Soil: Decoupling Biotic and Abiotic Processes. Water Air Soil Pollut. 228. https://doi.org/10.1007/s11270-017-3402-9.

Hurvich, C.M., Tsai, C.-L., 1989. Regression and time series model selection in small samples. Biometrika 76, 297–307. https://doi.org/10.1093/biomet/76.2.297.

Jekel, M., Dott, W., Bergmann, A., Dünnbier, U., Gnirß, R., Haist-Gulde, B., Ruhl, A.S., 2015. Selection of organic process and source indicator substances for the anthropogenically influenced water cycle. Chemosphere 125, 155–167. https://doi.org/10.1016/j.chemosphere.2014.12.025.

Katayama, A., Bhula, R., Burns, G.R., Carazo, E., Felsot, A., Hamilton, D., Wauchope, R. D., October 2009. Bioavailability of Xenobiotics in the Soil Environment. In: Reviews of Environmental Contamination and Toxicology. Springer, New York, pp. 1–86. https://doi.org/10.1007/978-1-4419-1352-4_1.

Kodešová, R., Grabic, R., Kočárek, M., Klement, A., Golovko, O., Fér, M., Jakšík, O, 2015. Pharmaceuticals\textquotesingle sorptions relative to properties of thirteen different

soils. Sci. Total Environ. 511, 435–443. https://doi.org/10.1016/j.scitotenv.2014.12.088.
Lara-Pérez, C., Leyva, E., Zermeño, B., Osorio, I., Montalvo, C., Moctezuma, E., 2020. Photocatalytic degradation of diclofenac sodium salt: adsorption and reaction kinetic studies. Environ. Earth Sci. 79. https://doi.org/10.1007/s12665-020-09017-z.
Lee, J., Seo, Y., Essington, M.E., 2014. Sorption and Transport of Veterinary Pharmaceuticals in Soil—A Laboratory Study. Soil Sci. Soc. Am. J. 78, 1531–1543. https://doi.org/10.2136/sssaj2013.11.0490.
Lees, K., Fitzsimons, M., Snape, J., Tappin, A., Comber, S., 2018. Soil sterilization methods for use in OECD 106: How effective are they? Chemosphere 209, 61–67. https://doi.org/10.1016/j.chemosphere.2018.06.073.
Leistra, M., Van der Linden, A.M., Boesten, J.J., Tiktak, A., Van den Berg, F., 2001. PEARL model for pesticide behavior and emissions in soil-plant systems. In: description of the processes in FOCUS PEARL, v 1.1. Alterra, p. 1. Tech. rep..
Lerner, H.H., 1975. Diatrizoic Acid. 137–167. https://doi.org/10.1016/S0099-5428(08)60011-8.
Li, J., Dodgen, L., Ye, Q., Gan, J., 2013. Degradation Kinetics and Metabolites of Carbamazepine in Soil. Environ. Sci. Technol. 47, 3678–3684. https://doi.org/10.1021/es304944c.
Lin, K., Gan, J., 2011. Sorption and degradation of wastewater-associated non-steroidal anti-inflammatory drugs and antibiotics in soils. Chemosphere 83, 240–246. https://doi.org/10.1016/j.chemosphere.2010.12.083.
Luo, Y., Guo, W., Ngo, H.H., Nghiem, L.D., Hai, F.I., Zhang, J., Wang, X.C., 2014. A review on the occurrence of micropollutants in the aquatic environment and their fate and removal during wastewater treatment. Sci. Total Environ. 473–474, 619–641. https://doi.org/10.1016/j.scitotenv.2013.12.065.
Luo, T., Chen, T., Boily, J.-F., Hanna, K., 2024. Mobility and transport of pharmaceuticals nalidixic acid and niflumic acid in saturated soil columns. Soil & Environmental Health 2, 100060. https://doi.org/10.1016/j.seh.2024.100060.
Maraqa, M.A., Khashan, S.A., 2014. Modeling solute transport affected by heterogeneous sorption kinetics using single-rate nonequilibrium approaches. J. Contam. Hydrol. 157, 73–86. https://doi.org/10.1016/j.jconhyd.2013.11.005.
Margot, J., Rossi, L., Barry, D.A., Holliger, C., 2015. A review of the fate of micropollutants in wastewater treatment plants. WIREs Water 2, 457–487. https://doi.org/10.1002/wat2.1090.
Martinez-Hernández, V., Meffe, R., López, S.H., de Bustamante, I., 2016. The role of sorption and biodegradation in the removal of acetaminophen, carbamazepine, caffeine, naproxen and sulfamethoxazole during soil contact: A kinetics study. Sci. Total Environ. 559, 232–241. https://doi.org/10.1016/j.scitotenv.2016.03.131.
MathWorks, 2023. MATLAB (Version R2023b) [Computer software]. https://www.mathworks.com/products/matlab.html.
Menacherry, S.P., Kodešová, R., Fedorova, G., Sadchenko, A., Kočárek, M., Klement, A., Grabic, R., 2023. Dissipation of twelve organic micropollutants in three different soils: Effect of soil characteristics and microbial composition. J. Hazard. Mater. 459, 132143. https://doi.org/10.1016/j.jhazmat.2023.132143.
Mirenga, E., Thiele-Bruhn, S., 2025. Sorption of Sulfonamide Antibiotics in Peat Soils With Different Properties. J. Plant Nutr. Soil Sci. 188 (3), 482. https://doi.org/10.1002/jpln.202400516.
Mora, A., Torres-Martínez, J. A., Capparelli, M. V., Zabala, A., & Mahlknecht, J, 2022. Effects of wastewater irrigation on groundwater quality: An overview. Current Opinion in Environmental Science & Health 25, 100322. https://doi.org/10.1016/j.coesh.2021.100322.
Mutavdžić Pavlović, D., Ćurković, L., Grčić, I., Šimić, I., Župan, J., 2017. Isotherm, kinetic, and thermodynamic study of ciprofloxacin sorption on sediments. Environ. Sci. Pollut. Res. 24 (10091–10), 106. https://doi.org/10.1007/s11356-017-8461-3.
Naylor, D., McClure, R., Jansson, J., 2022. Trends in Microbial Community Composition and Function by Soil Depth. Microorganisms 10, 540. https://doi.org/10.3390/microorganisms10030540.
Nguyen, M.-K., Lin, C., Nguyen, H.-L., Hung, N.T., La, D.D., Nguyen, X.H., Nguyen, D.D., 2023. Occurrence, fate, and potential risk of pharmaceutical pollutants in agriculture: Challenges and environmentally friendly solutions. Sci. Total Environ. 899, 165323. https://doi.org/10.1016/j.scitotenv.2023.165323.
Ofori, S., Abebrese, D.K., Růžičková, I., Wanner, J., 2024. Reuse of Treated Wastewater for Crop Irrigation: Water Suitability, Fertilization Potential, and Impact on Selected Soil Physicochemical Properties. Water 16, 484. https://doi.org/10.3390/w16030484.
Otte, J.M., Blackwell, N., Soos, V., Rughöft, S., Maisch, M., Kappler, A., Schmidt, C., 2018. Sterilization impacts on marine sediment—Are we able to inactivate microorganisms in environmental samples? FEMS Microbiol. Ecol. 94. https://doi.org/10.1093/femsec/fiy189.
Park, J., Huwe, B., 2016. Sorption of pharmaceuticals and personal care products (PPCPs) to a mineral soil: Effects of pH, ionic strength and anionic organic matter. Sci. Total Environ. 545–546, 331–338. https://doi.org/10.1016/j.envpol.2016.01.089.
Partyka, M.L., Bond, R.F., 2022. Wastewater reuse for irrigation of produce: A review of research, regulations, and risks. Sci. Total Environ. 828, 154385. https://doi.org/10.1016/j.scitotenv.2022.154385.
Paz, A., Tadmor, G., Malchi, T., Blotevogel, J., Borch, T., Polubesova, T., Chefetz, B., 2016. Fate of carbamazepine, its metabolites, and lamotrigine in soils irrigated with reclaimed wastewater: Sorption, leaching and plant uptake. Chemosphere 160, 22–29. https://doi.org/10.1016/j.chemosphere.2016.06.048.
Pérez-Lucas, G., Navarro, S., 2024. How Pharmaceutical Residues Occur, Behave, and Affect the Soil Environment. Journal of Xenobiotics 14, 1343–1377. https://doi.org/10.3390/jox14040076.
Peters, A., Durner, W., Iden, S., 2024. The PDI model system for parameterizing soil hydraulic properties. Vadose Zone J. 23 (4). https://doi.org/10.1002/vzj2.20338.
Prakathi, J., Mahanty, B., Lhamo, P., 2020. Adsorption, Bioavailability and Microbial Toxicity of Diclofenac in Agricultural Soil. Bull. Environ. Contam. Toxicol. 105, 490–495. https://doi.org/10.1007/s00128-020-02955-1.
Qin, Q., Chen, X., Zhuang, J., 2014. The Fate and Impact of Pharmaceuticals and Personal Care Products in Agricultural Soils Irrigated With Reclaimed Water. Crit. Rev. Environ. Sci. Technol. 45, 1379–1408. https://doi.org/10.1080/10643389.2014.955628.
Radolinski, J., Le, H., Hilaire, S.S., Xia, K., Scott, D., Stewart, R.D., 2022. A spectrum of preferential flow alters solute mobility in soils. Sci. Rep. 12. https://doi.org/10.1038/s41598-022-08241-w.
Rahman, M.M., Liedl, R., Grathwohl, P., 2004. Sorption kinetics during macropore transport of organic contaminants in soils: Laboratory experiments and analytical modeling. Water Resour. Res. 40. https://doi.org/10.1029/2002WR001946.
Ren, X., Zeng, G., Tang, L., Wang, J., Wan, J., Liu, Y., Deng, R., 2018. Sorption, transport and biodegradation – An insight into bioavailability of persistent organic pollutants in soil. Sci. Total Environ. 610–611, 1154–1163. https://doi.org/10.1016/j.scitotenv.2017.08.089.
Revitt, D.M., Balogh, T., Jones, H., 2015. Sorption behaviors and transport potentials for selected pharmaceuticals and triclosan in two sterilized soils. J. Soils Sediments 15, 594–606. https://doi.org/10.1007/s11368-014-1025-y.
Rietra, R.P., Berendsen, B.J., Mi-Gegotek, Y., Römkens, P.F., Pustjens, A.M., 2024. Prediction of the mobility and persistence of eight antibiotics based on soil characteristics. Heliyon 10, e23718. https://doi.org/10.1016/j.heliyon.2023.e23718.
Rodríguez-López, L., Santás-Miguel, V., Cela-Dablanca, R., Núñez-Delgado, A., Álvarez-Rodríguez, E., Pérez-Rodríguez, P., & Arias-Estévez, M, July 2022. Ciprofloxacin and Trimethoprim Adsorption/Desorption in Agricultural Soils. Int. J. Environ. Res. Public Health 19, 8426. https://doi.org/10.3390/ijerph19148426.
Rodríguez-López, L., Santás-Miguel, V., Cela-Dablanca, R., Núñez-Delgado, A., Álvarez-Rodríguez, E., Rodríguez-Seijo, A., Arias-Estévez, M., 2024. Sorption of Antibiotics in Agricultural Soils as a Function of pH. Spanish Journal of Soil Science 14. https://doi.org/10.3389/sjss.2024.12402.
Sandrin, S.K., Jordan, F.L., Maier, R.M., Brusseau, M.L., 2001. Biodegradation during contaminant transport in porous media: 4. Impact of microbial lag and bacterial cell growth. J. Contam. Hydrol. 50, 225–242. https://doi.org/10.1016/S0169-7722(01)00112-7.
Schaffer, M., Boxberger, N., Börnick, H., Licha, T., Worch, E., 2012. Sorption influenced transport of ionizable pharmaceuticals onto a natural sandy aquifer sediment at different pH. Chemosphere 87, 513–520. https://doi.org/10.1016/j.chemosphere.2011.12.053.
Scheurer, M., Storck, F.R., Graf, C., Brauch, H.-J., Ruck, W., Lev, O., Lange, F.T., 2011. Correlation of six anthropogenic markers in wastewater, surface water, bank filtrate, and soil aquifer treatment. J. Environ. Monit. 13, 966. https://doi.org/10.1039/C0EM00701C.
Schmidtová, Z., Kodešová, R., Grabicová, K., Kočárek, M., Fér, M., Švecová, H., Grabic, R., 2020. Competitive and synergic sorption of carbamazepine, citalopram, clindamycin, fexofenadine, irbesartan and sulfamethoxazole in seven soils. J. Contam. Hydrol. 234, 103680. https://doi.org/10.1016/j.jconhyd.2020.103680.
Schübl, M., Kiecak, A., Hug, K., Lintelmann, J., Zimmermann, R., Stumpp, C., 2021. Sorption and biodegradation parameters of selected pharmaceuticals in laboratory column experiments. J. Contam. Hydrol. 236, 103738. https://doi.org/10.1016/j.jconhyd.2020.103738.
Šimůnek, J., van Genuchten, M.T., 2008. Modeling Nonequilibrium Flow and Transport Processes Using HYDRUS. Vadose Zone J. 7, 782–797. https://doi.org/10.2136/vzj2007.0074.
Seelig, A.H., Junghans, V., Reemtsma, T., Zahn, D., 2025. Plant uptake of persistent and mobile chemicals in rocket (Eruca sativa)—A greenhouse study on agricultural wastewater reuse. Environ. Sci. Technol. 59 (18), 9265–9274. https://doi.org/10.1021/acs.est.5c02379.
Šimůnek, J., Šejna, M., Saito, H., Sakai, M., van Genuchten, M.T., 2013. The hydrus-1D software package for simulating the movement of water, heat, and multiple solutes in variably saturated media (version 4.17) [software]. https://www.pc-progress.com. The hydrus-1D software package for simulating the movement of water, heat, and multiple solutes in variably saturated media (version 4.17) [software]. https://www.pc-progress.com. Von https://www.pc-progress.com abgerufen.
Site, A.D., 2001. Factors Affecting Sorption of Organic Compounds in Natural Sorbent/Water Systems and Sorption Coefficients for Selected Pollutants. A Review. J. Phys. Chem. Ref. Data 30, 187–439. https://doi.org/10.1063/1.1347984.
Spain, J.C., Van Veld, P.A., 1983. Adaptation of Natural Microbial Communities to Degradation of Xenobiotic Compounds: Effects of Concentration, Exposure Time, Inoculum, and Chemical Structure. Appl. Environ. Microbiol. 45, 428–435. https://doi.org/10.1128/aem.45.2.428-435.1983.
Storck, F.R., Skark, C., Remmler, F., Brauch, H.-J., 2016. Environmental fate and behavior of acesulfame in laboratory experiments. Water Sci. Technol. 74, 2832–2842. https://doi.org/10.2166/wst.2016.452.
Strawn, D.G., 2021. Sorption Mechanisms of Chemicals in Soils. Soil Systems 5, 13. https://doi.org/10.3390/soilsystems5010013.
Streck, T., Poletika, N., Jury, W.A., Farmer, W.J., 1995. Description of Simazine Transport with Rate-Limited, Two-Stage, Linear and Nonlinear Sorption. Water Resour. Res. 31, 811–822. https://doi.org/10.1029/94WR02822.
Süßmuth, R., Shrestha, P., Navarrete, Andrea Diaz, C., Wege, F.-F., Achten, C., & Hennecke, D., 2024. Impact of different sterilization techniques on sorption and NER formation of test chemicals in soil. Chemosphere 357, 141915. https://doi.org/10.1016/j.chemosphere.2024.141915.

Thalmann, M., Neubert, L., Klitzke, S., Ruhl, A.S., Peters, A., 2025a. Sorption of Organic Micropollutants to an Agricultural Soil: Effect of Ionic Strength, Cation Valence and pH. Water Air Soil Pollut. 236. https://doi.org/10.1007/s11270-025-07885-4.

Thalmann, M., Hohenbrink, T.L., Klitzke, S., Ruhl, A.S., Peters, 2025b. A (under review). User-Friendly Tool for the Assessment of Groundwater Contamination Risks by Long-Term Irrigation with Reclaimed Water. Submitted to. J. Contam. Hydrol. Preprint available at https://doi.org/10.2139/ssrn.5231271.

Thelusmond, J.-R., Kawka, E., Strathmann, T.J., Cupples, A.M., 2018. Diclofenac, carbamazepine and triclocarban biodegradation in agricultural soils and the microorganisms and metabolic pathways affected. Sci. Total Environ. 640–641, 1393–1410. https://doi.org/10.1016/j.scitotenv.2018.05.403.

Thor, J., Dittmann, D., Meyer, A., Zeeshan, M., Johne, S., Reynaert, E., Ruhl, A.S., 2025. Transformation of persistent organic micropollutants by UV and UV/H2O2 in wastewater treatment plant effluent. Water Supply 25, 65–82. https://doi.org/10.2166/ws.2024.261.

Trevors, J.T., 1996. Sterilization and inhibition of microbial activity in soil. J. Microbiol. Methods 26, 53–59. https://doi.org/10.1016/0167-7012(96)00843-3.

USDA, 2017. Soil Survey Manual. In: United States Department of Agriculture Handbook, No. 18. Government Printing Office, Washington, DC.

van Genuchten, M.T., Wagenet, R.J., 1989. Two-Site/Two-Region Models for Pesticide Transport and Degradation: Theoretical Development and Analytical Solutions. Soil Sci. Soc. Am. J. 53, 1303–1310. https://doi.org/10.2136/sssaj1989.03615995005300050001x.

Wang, H., Li, X., Sun, Z., Cao, X., Zhang, J., Chen, Q., Ma, R., 2024. The Influence of pH on Sulfamethoxazole in Soil Systems: Migration and Degradation. Water, Air, & Soil Pollution 235. https://doi.org/10.1007/s11270-024-07530-6.

Williams, C.F., Williams, C.F., Adamsen, F.J., 2006. Sorption-Desorption of Carbamazepine from Irrigated Soils. J. Environ. Qual. 35, 1779–1783. https://doi.org/10.2134/jeq2005.0345.

Wu, L., Dai, J., Bi, E., 2020. Roles of dissolved humic acid and tannic acid in sorption of benzotriazole to a sandy loam soil. Ecotoxicol. Environ. Saf. 204, 111088. https://doi.org/10.1016/j.ecoenv.2020.111088.

Xu, J., Wu, L., Chang, A.C., 2009. Degradation and adsorption of selected pharmaceuticals and personal care products (PPCPs) in agricultural soils. Chemosphere 77, 1299–1305. https://doi.org/10.1016/j.chemosphere.2009.09.063.

Xu, B., Liu, F., Brookes, P.C., Xu, J., 2018. The sorption kinetics and isotherms of sulfamethoxazole with polyethylene microplastics. Mar. Pollut. Bull. 131, 191–196. https://doi.org/10.1016/j.marpolbul.2018.04.027.

Xu, Y., Yu, X., Xu, B., Peng, D., Guo, X., 2021. Sorption of pharmaceuticals and personal care products on soil and soil components: Influencing factors and mechanisms. Sci. Total Environ. 753, 141891. https://doi.org/10.1016/j.scitotenv.2020.141891.

Yamamoto, H., Nakamura, Y., Moriguchi, S., Nakamura, Y., Honda, Y., Tamura, I., Sekizawa, J., 2009. Persistence and partitioning of eight selected pharmaceuticals in the aquatic environment: Laboratory photolysis, biodegradation, and sorption experiments. Water Res. 43, 351–362. https://doi.org/10.1016/j.watres.2008.10.039.

Zeeshan, M., Schumann, P., Pabst, S., Ruhl, A.S., 2023. Transformation of potentially persistent and mobile organic micropollutants in column experiments. Heliyon 9, e15822. https://doi.org/10.1016/j.heliyon.2023.e15822.

Zhang, C., Barron, L., Sturzenbaum, S., 2021. The transportation, transformation and (bio)accumulation of pharmaceuticals in the terrestrial ecosystem. Sci. Total Environ. 781, 146684. https://doi.org/10.1016/j.scitotenv.2021.146684.